Chem Soc Rev

REVIEW ARTICLE

View Article Online
View Journal | View Issue

Cite this: *Chem. Soc. Rev.*, 2015, 44, 228

Zeolite-like metal–organic frameworks (ZMOFs): design, synthesis, and properties

Mohamed Eddaoudi,*[ab] Dorina F. Sava,[bc] Jarrod F. Eubank,[bd] Karim Adil[a] and Vincent Guillerm[a]

Received 8th July 2014

DOI: 10.1039/c4cs00230j

www.rsc.org/csr

This review highlights various design and synthesis approaches toward the construction of ZMOFs, which are metal–organic frameworks (MOFs) with topologies and, in some cases, features akin to traditional inorganic zeolites. The interest in this unique subset of MOFs is correlated with their exceptional characteristics arising from the periodic pore systems and distinctive cage-like cavities, in conjunction with modular intra- and/or extra-framework components, which ultimately allow for tailoring of the pore size, pore shape, and/or properties towards specific applications.

1. Introduction

In recent years, hybrid organic–inorganic materials, especially metal–organic frameworks (MOFs),[1] have developed rapidly due, in part, to their endlessly modular and versatile nature, which is evident from the numerous reported metal-ion or metal-cluster types in combination with a continuously expanding library of multi-functional organic ligands. In addition, MOFs, which vary in dimensionality from two- to three-periodic extended frameworks, including open, permanently porous structures, are efficiently generated through typically mild synthetic techniques, resulting in highly crystalline materials, ideal for in-depth characterization of their structures. As such, correlations have been drawn between their structure(s) and properties, indicating their outstanding potential in many applications (*e.g.*, gas storage/separation/sequestration, catalysis, sensing, magnetism, non-linear optics, and more).[2–14] In this context we see another key feature contributing to the precipitous advancement of MOFs, the potential for designing methods towards tailored functional materials.

Numerous rational approaches to target particular MOF structures have been devised and systematically developed over the past couple of decades. A major advancement is attributed to the molecular building block (MBB) approach,[15–23] an approach that views certain discrete components with known features as individual building blocks for the construction of a final structure; essentially, the effective coordination geometry of single-metal ions and/or inorganic clusters, as well as the shape of the corresponding multifunctional organic ligands, directs the MOF formation, usually based on known, targeted network topologies. This strategy offers a prospective avenue toward not only the design and construction of materials, but also designed functional materials, as desired functions/properties can be incorporated at the design (*i.e.*, building block) stage. For the primary construction of the targeted structures, it is necessary to utilize MBBs that possess rigidity and desired directionality prior to the assembly process. As the inorganic MBBs are typically formed *in situ*, it is fundamentally important to identify the appropriate reaction conditions under which they are consistently generated. Once this aspect is realized, desired frameworks can be targeted by a combination of the inorganic MBB and judiciously selected organic ligands (which may serve merely as bridging linkers or as additional rigid, directional MBBs, depending on the desired framework).[23]

One ideal type of structure to target is the group of purely inorganic materials known as zeolites, which represent a benchmark in the area of porous solid-state materials, owing this status to their notable commercial significance.[24] These materials are comprised of Si and/or Al tetrahedral metal ions (T), linked by oxygen atoms (O, technically oxide ions), at approximately 144° T–O–T angles. The attractiveness associated with these compounds relies, in part, on their porosity, with homogeneously-sized and -shaped openings and voids, and forbidden interpenetration. The confined spaces permit their conventional use *par excellence* as shape- and size-selective catalysts, ion exchangers (ion removal and water softening), adsorbents (separation and gas storage), *etc.*[24–37] The diversity

[a] *Functional Materials Design, Discovery and Development Research Group (FMD^3), Advanced Membranes and Porous Materials Center (AMPM), Division of Physical Sciences and Engineering, King Abdullah University of Science and Technology (KAUST), Thuwal 23955-6900, Kingdom of Saudi Arabia. E-mail: mohamed.eddaoudi@kaust.edu.sa*
[b] *Department of Chemistry, University of South Florida, 4202 East Fowler Ave., Tampa, FL 33620, USA*
[c] *Sandia National Laboratories, Nanoscale Sciences Department, Albuquerque, NM 87185, USA*
[d] *Department of Chemistry and Physics, Florida Southern College, Lakeland, FL 33801, USA*

of these compounds is reflected in the extended number of framework types (there are currently 225 zeolites, as recognized by the International Zeolites Association),[38] each differentiated by a specific profile, such as the size of member rings (MR), window/aperture opening, cage dimensions, charge density, framework density (FD, the number of tetrahedral vertices per 1000 Å^3), and types of pores. Thus, the access to a multitude of networks makes zeolite-like (also sometimes referred to as zeolitic, zeotype, or zeotypic) materials highly valuable in function. The diverse nature of these materials is often influenced by the synthetic conditions, and by the use of structure directing agents (SDAs). However, limitations in their design and tunability restrict these functional materials to certain pore sizes and, consequently, to smaller molecule applications. In addition, a general trend implies that increasing pore sizes may lead to unidimensional pore systems and, hence, limit the applications.

In this context, and considering the relevance of the functions associated with solid-state porous materials on a societal and industrial level, the pursuit of novel materials, like MOFs, based on, and expanding, zeolitic networks has become a prominent and encouraging avenue. Consequently, this *review* aims to portray the state-of-the-art in the emerging area of MOFs related to zeolite nets. The focus will be placed on the breadth and efficacy of design routes (Fig. 1), delineating avenues toward the construction of zeolite-like MOFs (ZMOFs):

(i) based on the ''edge-expansion'' of traditional zeolites;

(ii) assembled from hierarchically superior building units, such as metal–organic cubes, regarded as d4Rs in zeolites;

(iii) derived from enlarged tetrahedral building units; and

(iv) built *via* organic tetrahedral nodes.

The most prominent examples of each strategy are to be briefly outlined. The concluding outlook will summarize the advancements in this field, with emphasis on the potential of pertinent applications.

2. Design strategies and synthetic challenges

The construction of MOFs from MBBs has facilitated the process of design and has set necessary conditions for the assembly of targeted networks.[39] In particular, carboxylate-based metal clusters have proven effective at generating intended MBBs *in situ*, which has allowed access to expected, as well as novel, frameworks. Indeed, by gaining adequate control over these design tools, a new generation, an array, of novel materials has been pursued and detailed.[13,23,40–42] Among metal–organic assemblies, primary emphasis has been placed on 3-periodic nets due to their potential for applications. Analysis of the literature occurrences of 3-periodic MOFs supports that the most prevalent framework types are based on 4-connected nodes, such as **dia**, **nbo**, **cds**, and **lvt** (none of which are zeolitic).[43] These reference three-letter codes are generally associated with the structural features/building blocks of particular networks, as implemented by O'Keeffe.[44] In the context of this *review*, the topological identity of inorganic zeolites will be identified with uppercase three-letter codes (*e.g.*, RHO), as implemented by the IZA, while their metal–organic analogues will be expressed by the corresponding bold lowercase three-letter code (*e.g.*, **rho**). It should be noted that there are some cases where the three-letter codes are not the same for the IZA and the RCSR[44] (O'Keeffe) analogues (*e.g.*, BCT and **crb**, respectively).

Mohamed Eddaoudi

Mohamed Eddaoudi was born in Agadir, Morocco. He is currently Professor of Chemical Science and Associate Director of the Advanced Membranes and Porous Materials Center, King Abdullah University of Science and Technology (KAUST, Kingdom of Saudi Arabia). He received his PhD in Chemistry, Université Denis Diderot (Paris VII), France. After postdoctoral research (Arizona State University, University of Michigan), he started his independent academic career as Assistant Professor, University of South Florida (2002), Associate Professor (2008), Professor (2010). His research focuses on developing strategies, based on (super)-molecular building approaches (MBB, SBB, SBL), for rational construction of functional solid-state materials, namely MOFs. Their prospective uses include energy and environmental sustainability applications. Dr Eddaoudi's eminent contribution to the burgeoning field of MOFs is evident from his selection in 2014 as a Thomson Reuters Highly Cited Researcher.

Dorina F. Sava

Dorina Sava received her PhD in Materials Chemistry from the University of South Florida in 2009 under the supervision of Professor Mohamed Eddaoudi. She is currently a Senior Member of Technical Staff at Sandia National Laboratories in Albuquerque, NM, where she previously completed her postdoctoral work (2010–2013). Her research is focused on both the fundamental and applied aspects of materials for energy and environment-related applications. Of particular interest is exploiting metal–organic frameworks as tunable platforms for energy storage, luminescence, and sensing.

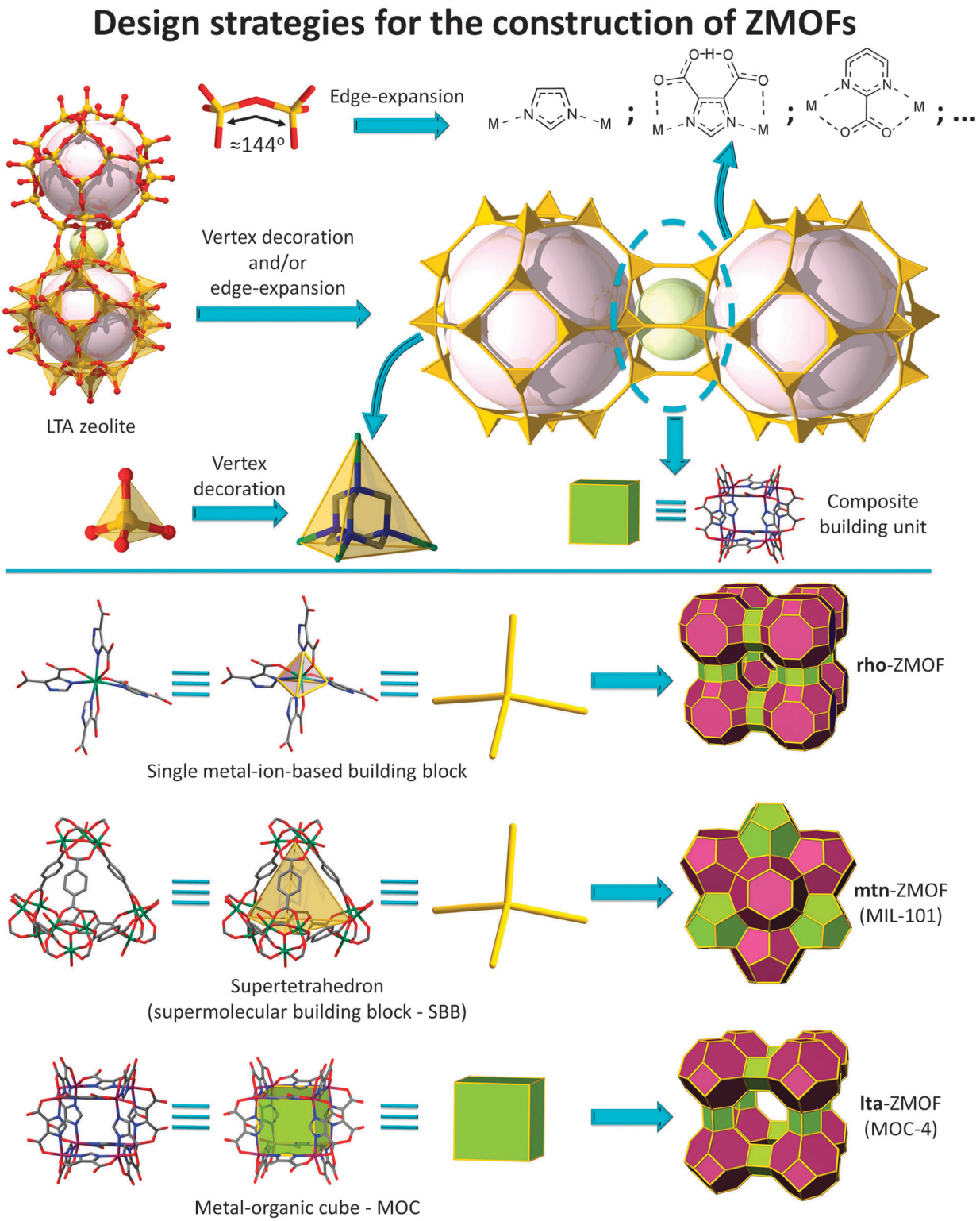

Fig. 1 Schematic representation of various design strategies for the construction of ZMOFs and MOFs with zeolitic features.

The rational construction of 4-connected, specifically tetrahedrally connected, porous materials, related in their topology and function to zeolites, with enlarged cavities and periodic intra- and/or extra-framework organic functionality, is an ongoing synthetic challenge, and it is of exceptional scientific and technological interest. The large and extra-large cavities offer great potential for innovative applications (serving as nanoreactors, becoming a platform for a variety of alternative applications pertaining to large molecules, nanotechnology, optics, sensor technology, and medicine, for example), enhancing

the correlation between structure and function. Within the last few years, MOFs with zeolitic topologies (ZMOFs)[15] have become a major focus for research groups in the materials chemistry community, who are particularly interested in the attractive properties associated with this unique subset of MOFs. Of particular interest, these materials inherently lack interpenetration (a feature that often affects the pores of would-be open MOFs); hence the accessibility to their porous channel systems is fully exploitable.

Expansion and/or decoration of tetrahedrally connected open networks, specifically zeolite-like nets, using the MBB approach provides the material designer with a prospective method to systematically construct functionalized porous materials with tunable and enlarged cavities by decorating the net and/or expanding the edges with a longer linker, or by substituting the tetrahedral vertices with larger supertetrahedral building units. To date, the synthesis of zeolite-like MOFs has proven to be more than trivial, as the complexity associated with these structures cannot be easily overcome. Moreover, the assembly of simple tetrahedral nodes correlates most often with the formation of the aforementioned **dia** (cubic diamond) topology, the so-called ''default'' structure for this type of node, which is not zeolitic.[45]

Therefore, multiple routes have been explored for targeting ''smarter'' tetrahedral building blocks, associated with the intended angle of connectivity in order to access non-default nets, and furthermore to generate MOFs with zeolite topologies. Amongst MOF analogues to zeolites, the sodalite (SOD, **sod**) net has the highest occurrence, as the structure accommodates a wide range for the T–O–T angle.[38] Over the years, other MOFs with zeolite-like topologies have been synthesized, such as **aco**,[46] **ana**,[47,48] **crb** (BCT),[47,49–61] **dft**,[47,49,62–64] **gis**,[47,49,59,65–70] **gme**,[47] **lta**,[71] **mer**,[47,49] **mtn**,[72–75] **sod**,[15,47–49,76–88] and **rho**,[15,47–49,87,88] but only recent studies consider an in-depth, systematic approach for the construction of these materials. Of those zeolitic networks targeted, the number of experimentally encountered frameworks can be considered limited. In order to access a larger number of zeolite-like frameworks, including unrevealed (*e.g.*, hypothetical) topologies; it is necessary to consider multiple variables, including SDAs and the nature of the tetrahedral or supertetrahedral building blocks, along with the angularity/additional functionality of the organic component. Theoretically, the number of possible structures to construct with these set conditions is yet vast, as reflected in the high number of zeolite-like networks from hypothetical databases.[89]

3. The edge-expansion approach to zeolite-like metal–organic frameworks (ZMOFs)

3.1. ZMOFs from angular ditopic N-donor ligands: pyrimidine-, imidazole-, and tetrazole-based linkers

The aim to construct functional hybrid solid-state porous materials with topologies akin to inorganic zeolites has been pursued by implementing a top-down, bottom-up approach. That is, by deconstructing the nets into small components, it is revealed that, as mentioned above, the materials are built from cationic, corner-sharing tetrahedra (T), bridged by an O^{2-} anion (with an average T–O–T angle in the range of $\sim$144°). ''Edge-expansion'' refers to a principle that consists of replacing the oxide ion with an organic functionality that preserves the intended angle of connectivity, and that is capable of rendering a material with similar features, only on an expanded scale.[88]

The original strategy is based on choosing single-metal ions with preferred tetrahedral geometry, in combination with angular ditopic N-donor organic ligands. Such candidates have been aromatic nitrogen heterocycle-based linkers such as imidazole, pyrimidine, or tetrazole molecules, and some relevant paradigms are briefly outlined in this section.

One of the earliest examples is reflected in the work of Keller, in 1997,[90] where the potential offered by pyrimidine ligands to afford crystalline materials with structures and properties related to porous inorganic materials is considered. In this instance, the compound reported is based on tetrahedral copper(I) centers coordinated by four pyrimidine molecules, and where BF_4^- anions are ensuring the charge balance of the assembly. The 3-periodic net has **pcl** (paracelsian) topology, consisting of 4-, 6- and 8-MRs, possessing structural features closely related to the ones observed in the feldspar material family, a group of silicate minerals. This early reference is of great importance, as it clearly delineates the use of intended organic ligands as potential mediators for the synthesis of metal–organic analogues of zeolites.

The same year brings a report of an interesting material also derived from a pyrimidine derivative, namely 2-amino-5-bromopyrimidine, yielding an early relevant example of a MOF with a true zeolite-like topology. The structure consists of copper(II) metal ions, with slightly distorted tetrahedral geometry, that are bridged by bromide ions, in addition to coordination to the organic moieties (*i.e.*, each copper forms two coordination bonds with two nitrogen atoms of the pyrimidine ligands, along with two other bonds with two bromide anions). The resulting 3-periodic framework possesses **crb** (BCT) zeolitic topology (Fig. 2) with unidimensional channels consisting of alternating cavities, one in which the amino groups are pointing to its interior (5.223 Å point to point, not considering the van der Waals (vdW) radii of the nearest atoms), while the other has the corresponding bromo-functional groups positioned inside the rather inaccessible cavity (3.695 Å point to point).

Given these guidelines, subsequent paradigms outline derivations of the approach described above. One example of a MOF with **sod** topology was reported by Tabares *et al.* in 2001, where 2-hydroxypyrimidine (2-Hpymo) organic ligands are bridging square planar copper(II) metal ion centers to construct the 3-periodic net.[79] Although the framework exhibits neutral characteristics, the authors delineate the selectivity of the material with regard to the salt or the ion pair, AX (where A = NH_4^+, Li^+, K^+, or Rb^+ and X = ClO_4^-, BF_4^-, or PF_6^-), recognition. The flexibility of the material is also mentioned, as it undergoes a reversible phase transformation, from a rhombohedral to a cubic phase upon immersion in a MeOH–H_2O solution.[79]

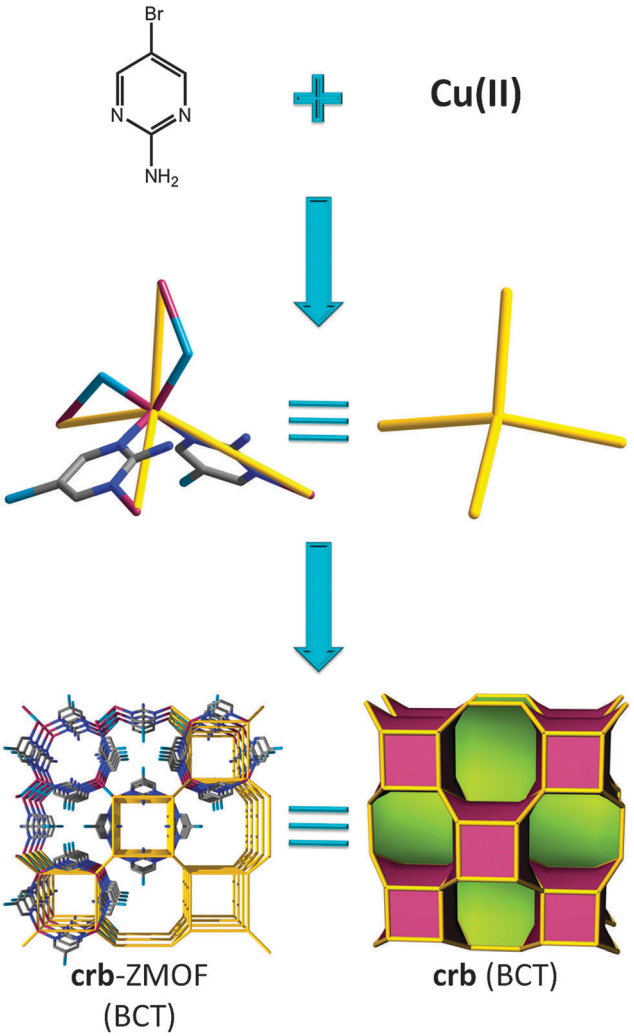

Fig. 2 Combination of 2-amino-5-bromo-pyrimidine ligand, bromide, and tetrahedrally coordinated copper (CuN_2Br_2) leads to a MOF with **crb** (BCT) topology.

Subsequently, a complete set of studies pertinent to gas sorption properties (hydrogen, nitrogen and carbon dioxide) were further evaluated for the parent copper-based material, as well as a palladium analogue, characterized by BET surface areas of 350 $m^2\ g^{-1}$ and 600 $m^2\ g^{-1}$, respectively.[91]

Correspondingly, a topologically equivalent net was constructed from yet another pyrimidine derivative, 4-hydroxypyrimidine (4-Hpymo) and copper(II), with octahedral geometry.[83] In spite of the obvious structural and topological similarities between the two materials (Fig. 3), the affinity towards salt recognition is not encountered in this instance, along with a reduced surface area, 65 $m^2\ g^{-1}$. Thus, the structural features, such as the orientation of the hydroxyl moiety, are greatly affecting the properties (*e.g.*, hydrophilicity or hydrophobicity of the pores) and the capabilities associated with these materials.

Imidazole and its derivatives have also been utilized as linkers to generate open frameworks resembling zeolite nets. An early example comes from the work of Trotter *et al.* in 1999, with studies focusing on the long-range ferromagnetic interactions at low temperatures of methylimidazolate and triazolate complexes.[52]

Interestingly, one of the compounds reported, based on an imidazole derivative, yields a 3-periodic ZMOF. Reaction between ferrocene and 2-methylimidazole results in tetrahedral iron-metal ion nodes, which, in conjunction with the organic linker, afford a material with **crb** (BCT) zeolitic topology. The uniperiodic channels accommodate ferrocene molecules.[52]

Furthermore, in 2001, Sironi and co-workers reported a series of polymorphs constructed from copper and imidazole. Among the supramolecular isomers, with 1 : 2 metal to ligand stoichiometry, a compound with **sod** topology (Fig. 4) is accounted.[78] The framework exhibits small unidimensional channels, 7.8 Å × 5.8 Å, distances measured point to point without considering the vdW radii of the nearest atoms.

Although valuable examples, the two compounds detailed above were not deliberately targeted as conceptual means to yield materials that mimic inorganic zeolite topologies. However, soon after, in 2002, Lee *et al.* emphasized the importance of the geometric attributes of this linker, and its capability to yield zeolite-like MOFs.[92] Their work evidences the potential offered by imidazolates to facilitate the synthesis of non-default MOFs based on tetrahedral nodes. The authors report on the synthesis of a compound derived from tetrahedral cobalt(II) metal ions, coordinated by four imidazole units, resulting in a 3-periodic net with **nog** topology. In spite of possessing zeolite-like features, the structure is not very open and its functionality is limited as a result of its structural features, an observation also valid for the previously discussed imidazolate-based MOFs.

Later studies conducted by Yaghi and co-workers,[47,49] among others,[48,63,82] further reinforce the ability of imidazole-based linkers to yield MOFs with zeolitic topologies and properties. Synthetically, a challenge is associated with the corresponding frameworks; they are neutral, which affects the reaction environment by limiting the ability to utilize SDAs, thus limiting the variety of the zeolite-like topologies that can be derived solely from imidazole. An alternative route in favor of structure diversity is portrayed by linker functionalization (*i.e.*, imidazole derivatives). In accordance with this approach, Yaghi *et al.* report on the synthesis of various ZMOFs, specifically referred to as zeolitic imidazolate frameworks (ZIFs), including **ana**, **crb** (BCT), **dft**, **gme**, **gis**, **lta**, **mer**, **sod** and **rho**.[93] The overall topological features resemble the ones encountered in the traditional inorganic zeolites, however on a larger scale, as a result of the aforementioned edge-expansion (*i.e.*, replacing the O ion with the angular imidazolate organic ligand).

When using benzimidazole, two materials with zeolitic **sod** and **rho** topologies are obtained; however, by replacing the carbon atom with a nitrogen atom in the 4-position of benzimidazole, the ubiquitous diamond structure is favored, which highlights the difficulty of synthetically avoiding this default topology. Conversely, by replacing the carbon atom(s) with a nitrogen atom(s) in 5- or 5- and 7-positions on benzimidazole, a framework with **lta** (LTA, Linde type A, or zeolite A) topology is constructed, consisting of two types of cages, truncated cuboctahedra (α cage) and truncated octahedra (β cage) (Fig. 5).[71]

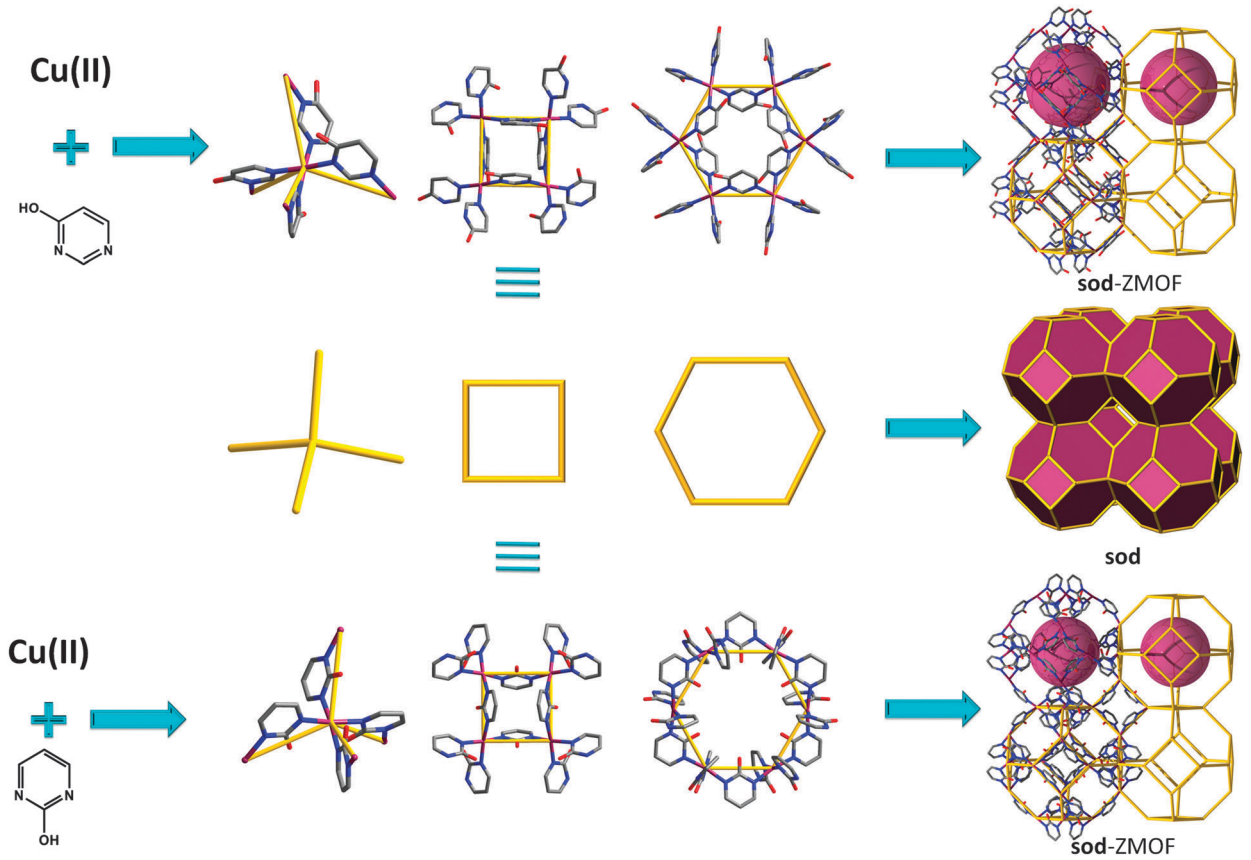

Fig. 3 Examples of **sod**-like frameworks based on 2-Hpymo (top) and 4-Hpymo (bottom): representative tetrahedral building units (TBUs), 4- and 6-MRs, periodically assembled for the construction of the repeating β-cage (schematically depicted in gold).

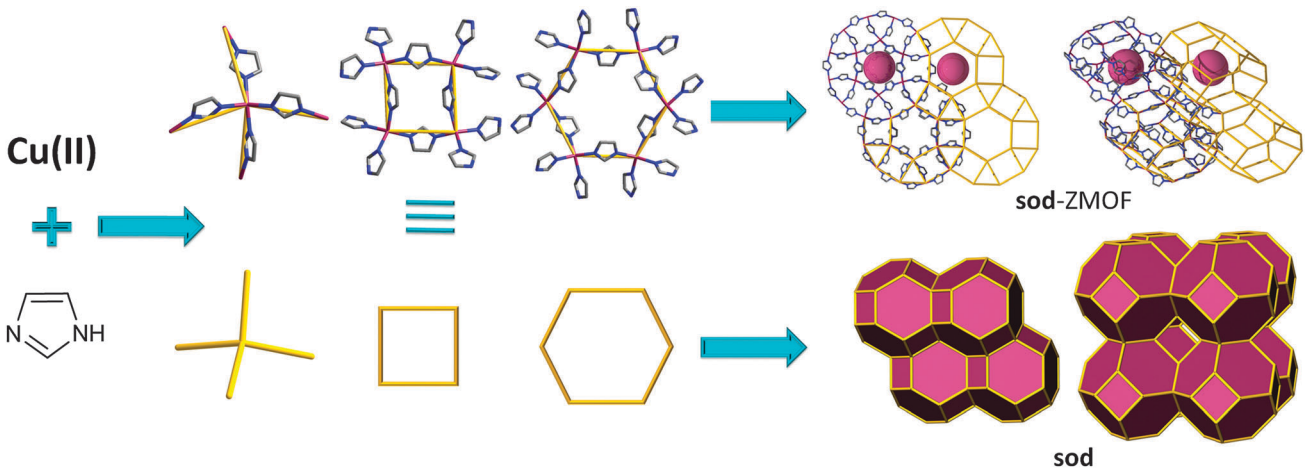

Fig. 4 Examples of **sod**-like framework based on Cu-imidazolate: Representative TBU, 4- and 6-MRs, periodically assembled for the construction of the repeating β-cage (schematically depicted in gold). Net with **sod**-like topology.

In contrast, this result demonstrates the potential effectiveness of organic ligand functionalization, as access to hierarchically complex structures with more than one type of cage remains a challenge. The inorganic LTA material has an internal free diameter of 11.4 Å, while in its metal–organic analogue, it increases to 15.4 Å. The material exhibits accessible porosity as evidenced by Ar, H_2, CO_2, and CH_4 gas sorption studies, possessing an estimated Langmuir surface area of 800 $m^2\ g^{-1}$. Hydrogen, carbon dioxide, and methane sorption studies were performed, and the potential for gas separation (CO_2–CH_4 mixtures) has also been investigated.

Additionally, this approach allows access to compounds possessing unprecedented zeolite-like features and extra-large cavities.

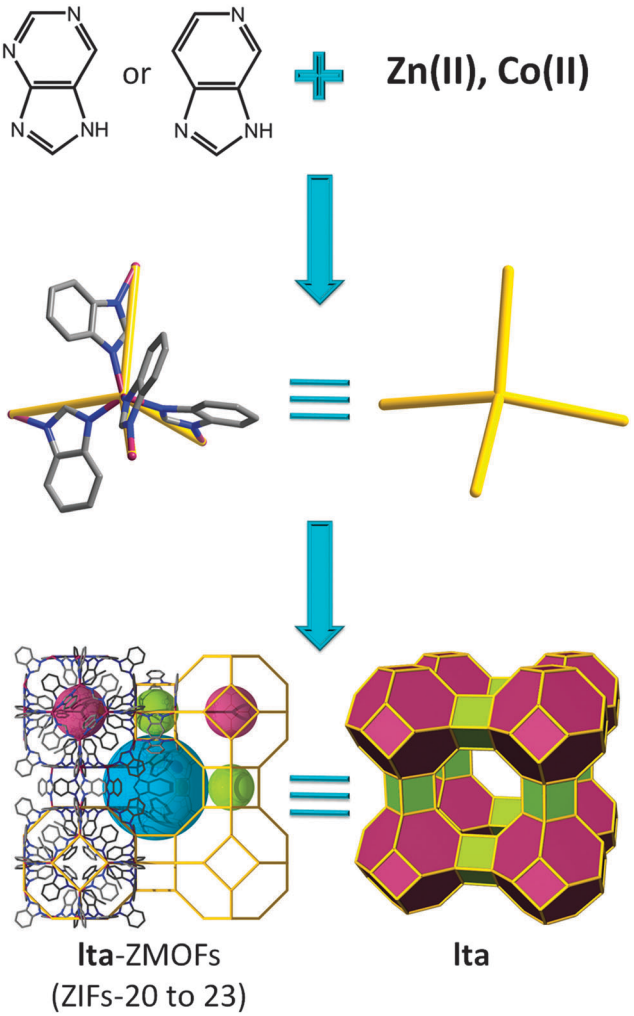

Fig. 5 Examples of organic linkers, 5-azabenzimidazolate and purinate, capable of producing a ZMOF net based on **lta** topology.

Two examples of such materials are ZIF-95 and ZIF-100, generically termed **poz** (ZIF-95) and **moz** (ZIF-100).[94] The first compound encompasses four different types of cages, two having impressive dimensions: **poz** A with accessible pore sizes of 25.1 Å × 14.3 Å and poz B, 30.1 Å × 20 Å; similarly, **moz** is constructed from cages that have up to 35.6 Å internal exploitable voids. Their estimated Langmuir surface areas are 1240 $m^2\ g^{-1}$ and 780 $m^2\ g^{-1}$, respectively, values much larger than the ones encountered for zeolite materials. The evaluation of the gas sorption related properties revealed that both materials selectively retain CO_2 in the pores in 50 : 50 CO_2/N_2, CO_2/CH_4, or CO_2/CO mixtures.

To access additional ZIF structures,[47] high throughput synthesis, a method inspired by similar techniques for testing pharmacology products, was implemented.[95] Introducing mixed organic ligands in the synthesis leads to the complementation of the conventional synthetic approaches. This approach has permitted the production of a multitude of materials based on tetrahedral nodes, including the default diamond structure, along with desired zeolite-like compounds, some previously synthesized through standard methods.

Another way to construct new imidazole-based zeolitic MOFs is to take advantage of the easy formation of tetrahedral M^{2+}-imidazole chemical bonds to design new imidazole-based ligands that can react as larger building blocks. Sun *et al.* reported a Co-based ZMOF built up from a novel, rigid 3-imidazole-containing ligand, 1,3,5-tri(1*H*-imidazol-4-yl)benzene. The structure is a binodal, (4,4)-connected (*i.e.*, (Co-ligand)-connected), porous net displaying a zeolitic **bct** topology.[96]

A similar concept was used to develop a "lightweight" version of ZIFs, referred to as zeolitic boron imidazolate frameworks (BIFs). Zeolite-like nets were targeted from predetermined tetrahedral boron-imidazolate complexes (from imidazole or imidazole derivatives).[97] These complexes are synthesized prior to the MOF process and then are further linked by monovalent cations (such as Li and Cu) into extended nets. For the creation of four-connected topologies from these complexes, the authors used a strategy similar to the one that led to the discovery of microporous $AlPO_4$ by analogy with porous silica. Just as Al^{3+} and P^{5+} ions can replace two Si^{4+} sites in a porous silicalite, Li^+ and B^{3+} can replace two Zn^{2+} sites in a $Zn(im)_2$ ZMOF framework (Fig. 6). The strategy affords materials with zeolitic topologies (**sod**), but also other types of 4-connected nets.[98] In some cases, the boron-imidazolate precursors are 3-connected, resulting in mixed 3,4-connected nets, or materials solely based on nodes of 3-connectivity. It is worth mentioning that Leoni *et al.* have predicted and studied the stability of 30 topologically different BIFs by DFT calculations, and have concluded that the **fau**, **rho**, and **gme** nets are the most promising candidates for hydrogen storage applications.[99]

One drawback of BIF materials comes from the short B–N distance bond (~1.5 Å) that implies a closer contact and stronger steric repulsion between imidazolate bridges, making the tunability

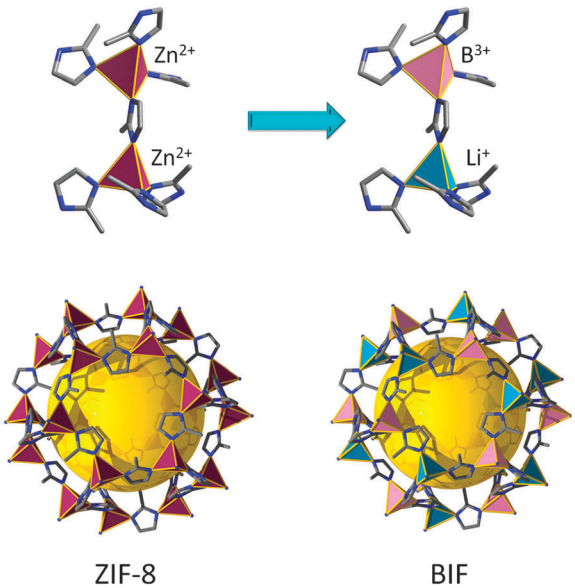

Fig. 6 Charge substitution from ZIFs to BIFs. Top: Zinc are purple tetrahedra, lithium are blue tetrahedra, boron are pink tetrahedra. Carbon and nitrogen are, respectively, gray and blue. Bottom: Analogy between the ZIF-8 and BIF, both displaying a **sod** topology.

of the framework challenging. Hence, Feng *et al.* have developed a new series of materials based only on 4-connected lithium nodes (Li–N ~ 2.0 Å) using a mixed-ligand strategy.[100] It should be noted that the total charge of the resultant 4-connected framework would be negative, if B^{3+}/Li^{+} is replaced with Li^{+}/Li^{+} and no change is made in the imidazolate ligands.[100] Accordingly, half of the negatively charged imidazolate ligands were replaced by neutral ligands, giving rise to new materials, named MVLIF-1 and MVLIF-2 (MVLIF stands for mixed valent ligand lithium imidazolate framework), that display non-zeolitic 4-connected topologies, **qzd** and **dia**, respectively.

As mentioned for some of the imidazolate-based ZMOFs, and evidenced by the incredible number of studies reported in this field, one of the most promising applications for MOF materials is gas adsorption. Long *et al.*,[101,102] among others,[103,104] have developed a series of **sod**-like materials from yet another promising type of N-donor ligand, a tetrazolate (in this case, 1,3,5-benzenetristetrazolate (BTT)), and investigated hydrogen adsorption properties.[105] The structure consists of six tetranuclear chloride-centered metal–tetrazolate clusters ($M_4(\mu^4\text{-Cl})L_8$, M = Cu(II), Fe(II), Co(II)), square units (like square faces) connected to and through eight triangular BTT ligands, forming a truncated octahedral sodalite-like cage (with an internal diameter of approximately 10.3 Å). The high concentration of exposed metal cations present within this framework makes it possible to reach a total storage capacity of 1.1 wt% and 8.4 g L^{-1} at 100 bar and 298 K (for the Fe-based analogue), associated with an initial isosteric heat of adsorption of 11.9 kJ mol^{-1}. It should be noted that, in recent years, sodalite-like analogues (some based on oxo-centered clusters) have been synthesized from pyrazole,[106] triazole,[107] and BTC (and expanded) derivatives.[108–113]

Recently, important efforts have been dedicated to developing new materials for the capture and storage of greenhouses gases, such as CO_2.[114–116] Many strategies to enhance carbon dioxide adsorption have been introduced, such as the use of coordinatively unsaturated metal centers,[40,117] the optimization of the pore size[118,119] or incorporation of alkylamines.[107,120–122] A third approach to increase CO_2 adsorbent amounts is the presence of amine-functionalized aromatic linkers.[123,124] Lan *et al.* have investigated the impact of the utilization of a N-rich aromatic ligand (without NH_2 groups) by fabricating a **sod**-ZMOF (Fig. 7) based on another tetrazolate linker that also incorporates an imidazole-like, triazole core (4,5-di-(1*H*-tetrazol-5-yl)-2*H*-1,2,3-triazol); this zeolitic framework demonstrates the achievement of high uptake capacity for CO_2, even in the absence of primary amines and open metal sites.[125]

To conclude this subchapter, it becomes apparent that the use of non-linear N-based ditopic or polytopic linkers, in conjunction with appropriate metal ion coordination geometry, successfully qualifies for the synthesis of MOFs with structures and functions closely related to zeolites. The identity of the linker, accompanied by various functional groups, influences the structural diversity and tunability of the materials.

3.2. ZMOFs constructed from the single-metal-ion-based MBB approach

Meanwhile, another approach to zeolite-like metal–organic frameworks was developed by our group, implementing a single-metal-ion-based MBB approach, which focused on the introduction of a higher degree of information at the single-metal ion level, which is crafting "smarter" predetermined building blocks.[15,88] The concept involved the use of organic ligands, like and including imidazolates, that have angular N-donors, but also must include secondary donors, such as O-donors; together the N- and O-donors form heterochelating moieties (*e.g.*, the nitrogen atom is positioned on the aromatic part of the ring, having carboxylates located in the α-position relative to the nitrogen).

The main advantage of this approach as compared to solely carboxylic acid or nitrogen-based ligands is the rigidity and directionality reinforced by the chelating ring that locks the metal in its position and maintains the geometric requirements that facilitate the design of targeted frameworks. Within the net-to-be, the nitrogen atoms direct the topology (*i.e.*, angular), while the carboxylates lock the metal in its position. Hence, the main attributes of this approach are the rigidity and the directionality embedded in these single-metal-ion based MBBs, which preserve the geometric specificities of the organic ligands utilized.

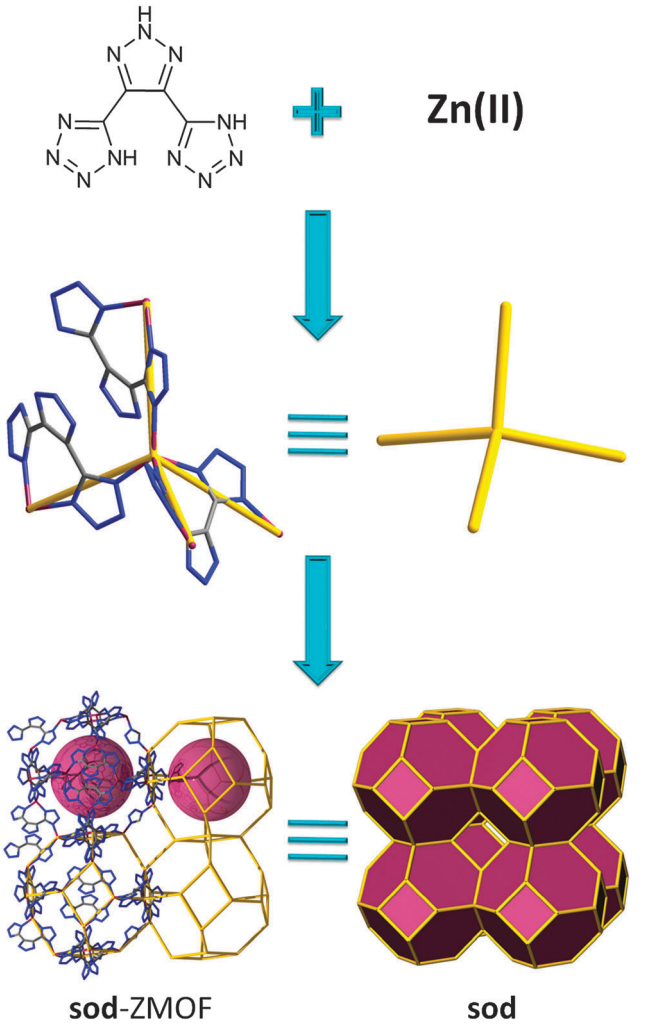

Fig. 7 Utilization of N-rich aromatic linker for the construction of a zinc-based ZMOF with **sod** topology.

The polytopic nature of such ligands has the leading role as to fully saturate the coordination sphere of the single-metal ion, in such a way that it precludes coordination of unwanted solvent or guest molecules. The hetero-functionality provided by the organic ligands results in the generation of MBBs of the type $MN_x(O_2C–)_y$ (where x represents participating angular N donors, typically involved in a ring of chelation, while y is translated to the additional carboxylate functionalities (often O-chelating) that complete the coordination sphere at the available metal sites; M is typically a 6-, 7-, or 8-coordinate metal ion).[126–128]

As such, the single-metal-ion-based MBB approach was quickly realized as a suitable method for targeting ZMOFs.[15,87,88] In addition to those zeolitic MOFs mentioned above, our ZMOFs represent a unique subset that is not only topologically related to the purely inorganic zeolites, but also exhibits similar properties:

(i) forbidden self-interpenetration, which permits the design of readily accessible extra-large cavities;

(ii) chemical stability, where the structural integrity is maintained in water (a feature not commonly encountered in MOFs), and allows for ZMOF applications for heterogeneous catalysis, separations, and sensors, especially in aqueous media;

(iii) anionic ZMOFs possess the ability to control and tune extra-framework cations toward specific applications such as catalysis, gas storage, the removal/sequestration of toxic metal ions, *etc.*

As with some of the previously mentioned approaches, this method involves edge-expansion of zeolite-like nets toward the design and synthesis of very open ZMOFs. The key factors are related to the ability to generate rigid and directional single-metal-ion-based MBBs that serve as the tetrahedral nodes (T) or tetrahedral building units (TBUs), which are to be positioned and locked at the intended angle, through the aid of the pre-designed heterofunctional organic ligands (concept schematically depicted in Fig. 8).

Therefore, non-default structures for the assembly of TBUs, such as zeolites, can be more easily targeted by judicious selection of the appropriately shaped rigid MBBs and linkers. Consequently, it is evident that introducing information into the MBB is vital, and it is of broad interest to use the MBB approach, based on rigid and directional single-metal-ion TBUs, as a solid platform and basis for developing new design strategies to construct and functionalize novel ZMOFs for specific applications.

Our approach allows for the preferential targeting of anionic ZMOFs, allowing for the utilization of different SDAs, suggesting that this strategy has little limitations in terms of the range of materials that it can generate. As in zeolite systems, the role played by SDAs in MOF systems enhances their potential for diversity, as has been previously demonstrated with the synthesis of supramolecular isomers derived from indium metal ions, 2,5-pyridinedicarboxylic acid (H_2PDC), and different SDAs: a discrete octahedron,[126] a 2D layered Kagomé structure,[126] and a 3D diamondoid net.[127] The same method has been utilized to target other metal–organic polyhedra (MOPs), like metal–organic cubes.[128–130]

In addition, in contrast to most zeolites, and along with green chemistry concepts, the synthesis of our ZMOFs is performed under mild conditions, which also permits the conservation of the structural integrity of the organic components.

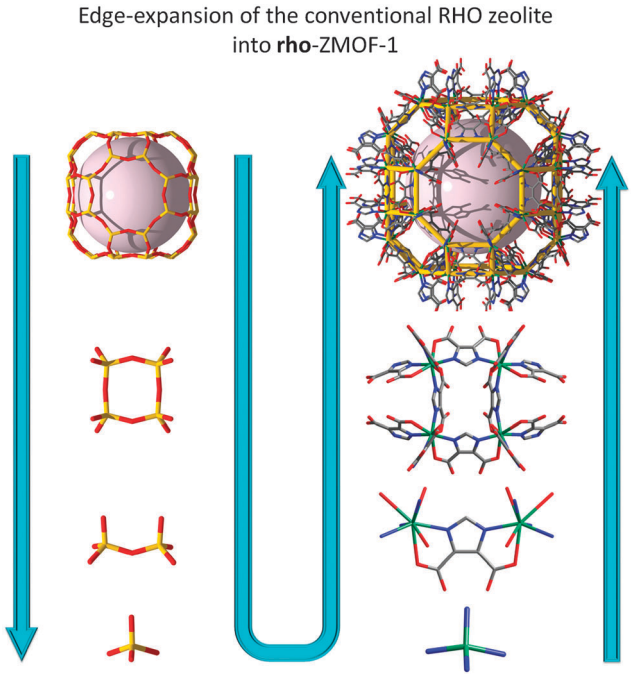

Fig. 8 Illustration of the edge-expansion strategy for the construction of a metal–organic analogue of zeolite RHO (specifically based on the α-cage).

Based on the single-metal-ion MBB conditions (possessing both desired angularities and heterofunctionality), imidazole-dicarboxylates and pyrimidinecarboxylates represent potential attractive candidates for targeting the desired ZMOFs.[15,87,88] From a metal ion choice perspective, those metals that have primarily six to eight available coordination sites are targeted (although a higher number of sites can be utilized as well), ions that should allow the formation of the intended building blocks of the type $MN_4(O_2C–)_2$, $MN_2(O_2C–)_4$, $MN_4(O_2C–)_4$, or $MN_2(O_2C–)_6$, to ultimately render MN_4 or $MN_2(O_2C–)_2$ directing units, all capable of being translated into TBUs.

According to these criteria, 4,5-imidazoledicarboxylic acid, H_3ImDC, is well-suited to target MOFs with zeolite-like topologies, since it concurrently possesses two N-,O-hetero-chelating moieties with a potential angle of 144° (directed by the M–N coordination). Additionally, if four HImDC ligands saturate each single-metal ion coordination sphere (divalent or trivalent), an anionic ZMOF can be realized. As in the 2,5-H_2PDC-based supramolecular isomers mentioned previously, the anionic nature allows for the utilization of cationic SDAs, as well as the exploration of applications akin to traditional zeolites (*e.g.*, ion exchange).

A reaction between $In(NO_3)_3{\cdot}5H_2O$ and H_3ImDC, in the presence of different SDAs does, in fact, yield different ZMOFs (Fig. 9).[15,88] Specifically, imidazole (HIm) leads to a **sod**-ZMOF, while 1,3,4,6,7,8-hexahydro-2*H*-pyrimido[1,2-*a*]pyrimidine (HPP) yields **rho**-ZMOF-1, where both materials possess volumes up to 8 times larger than their inorganic analogues. In the In-HImDC **sod**-ZMOF-1, each 6-coordinate In^{3+} ion is hetero-chelated by

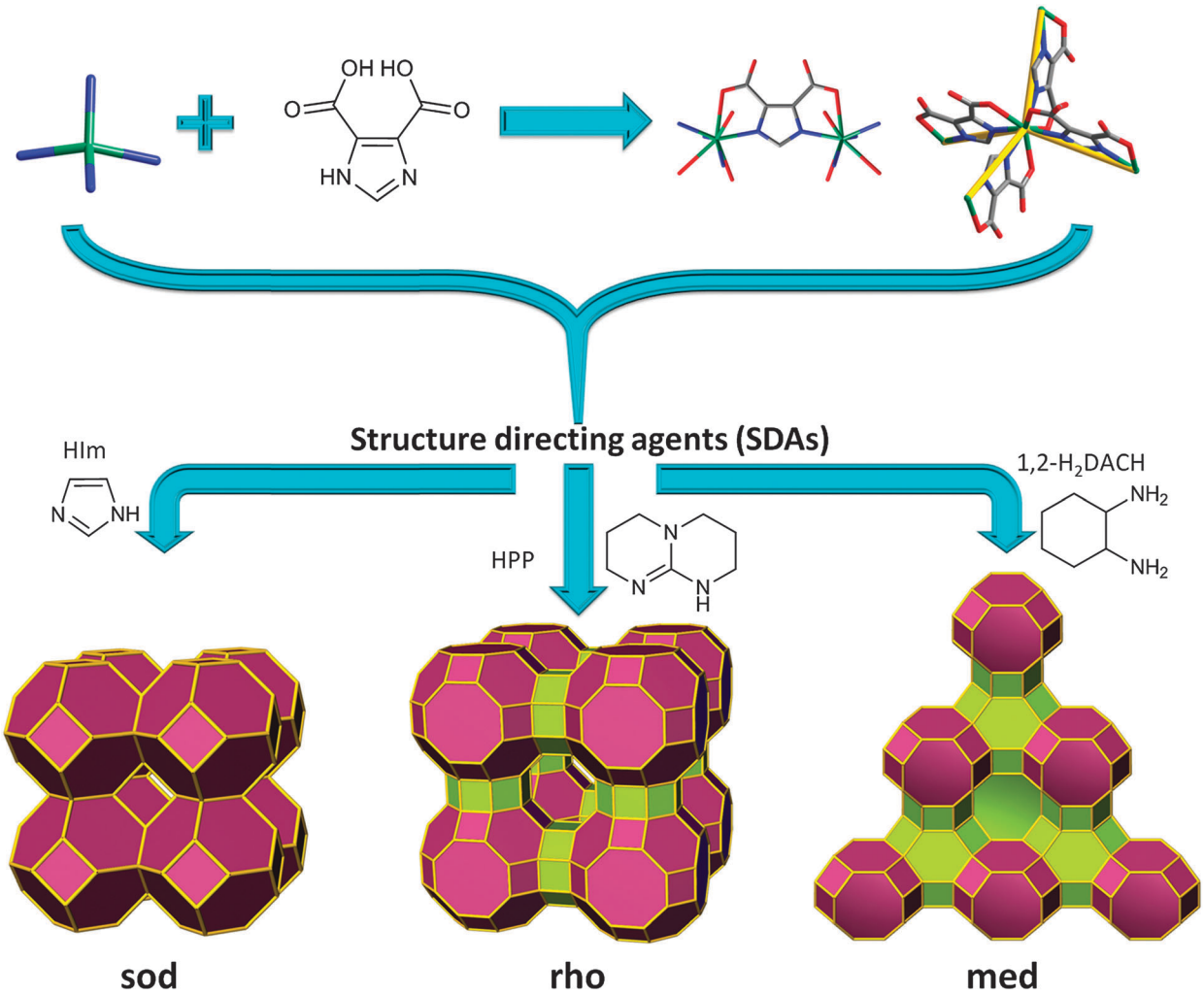

Fig. 9 Single-metal-ion-based MBB approach evidencing structural diversity in ZMOFs *via* SDAs (*i.e.*, directed synthesis).

two $HImDC^{2-}$ ligands and coordinated by the ancillary nitrogen-donor from two other $HImDC^{2-}$ ligands, resulting in the desired $InN_4(O_2C–)_2$ MBBs (InN_4 TBUs). In **rho**-ZMOF-1, each single-indium ion is 8-coordinate, saturated by the hetero-chelation of four $HImDC^{2-}$ ligands to give the intended $InN_4(O_2C–)_4$ MBBs (InN_4 TBUs). This anionic **rho**-ZMOF-1 was the first material ever to contain an organic component and have a zeolite RHO topology.

Unlike inorganic RHO zeolite and other RHO analogues, **rho**-ZMOF-1 requires twice as many positive charges, 48 (24 doubly protonated HPP molecules) *vs.* 24, to neutralize the anionic framework. Also, the extra-large cavities can accommodate a sphere of 18.2 Å in diameter inside each cage, outlining a benefit from edge-expansion of the aluminosilicate analogue evident by the doubling (3.10 nm *vs.* 1.51 nm) of the unit cell. In addition, the **sod**-ZMOF-1 represents the first example of a MOF with an anionic framework based on the **sod** topology, although some other examples of neutral or cationic sodalite-like MOFs have been synthesized previously, as detailed above.[15,88]

Additionally, our group's findings lead to the discovery of a novel zeolite-like net, **usf**-ZMOF (Fig. 10),[131] with an unprecedented topology at the time of its synthesis; independently, the topological data were reported in one of the hypothetical zeolite databases by the time of publication, and now it is referred to in the RCSR database as **med** topology. The synthetic protocol involves similar reagents as for **sod**-ZMOF-1 and **rho**-ZMOF-1 detailed above, yet in the presence of a different SDA, 1,2-diaminocyclohexane (1,2-H_2DACH). Each indium metal ion is coordinated to four nitrogen atoms and four oxygen atoms of four separate HImDC ligands, respectively, to form an eight-coordinate MBB, $InN_4(O_2C–)_4$, (InN_4 TBUs). The anionic nature of **usf**-ZMOF is neutralized by 40 doubly protonated 1,2-DACH molecules, accommodated by a unit cell with a volume (45 245 $Å^3$) that is 9.55 times higher than its analogous yet-to-be-constructed zeolite (4735 $Å^3$).

Given the anionic nature of our ZMOFs, a diverse range of applications is exploitable. The zeolite-like nature favors facile ion exchange capability of the organic cations in the cavities. To demonstrate, **rho**-ZMOF-1 was utilized, and it was found that the counter cations can be fully replaced at room temperature after 15 to 24 hours (depending on the inorganic cation used); the fully exchanged compounds retain their morphology and crystallinity. In a recent study, the effect of several extra-framework cations (as-synthesized sample, containing dimethylammonium cations,

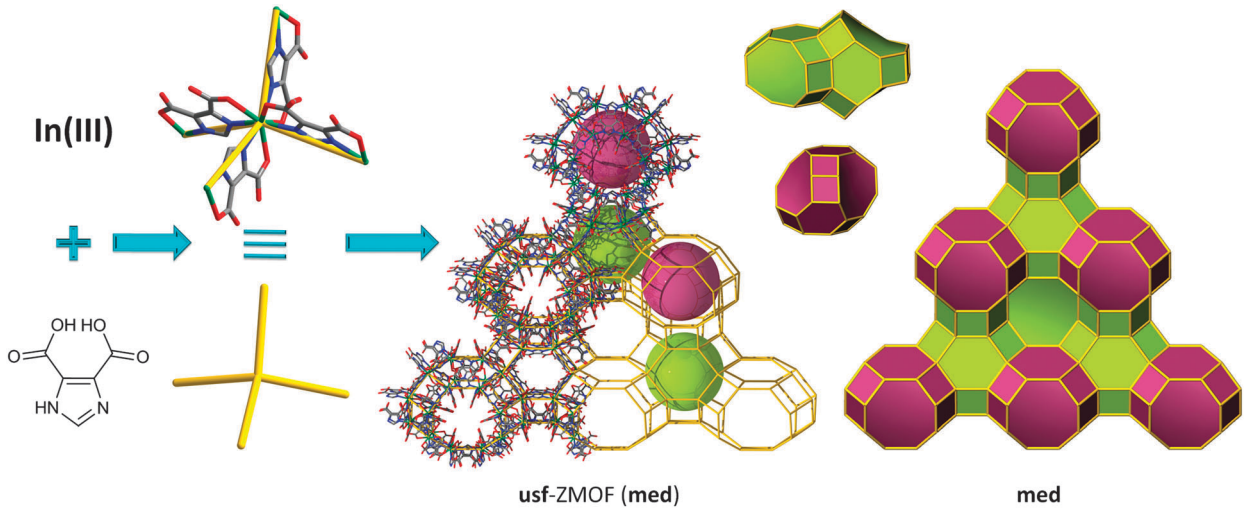

Fig. 10 Structural and tiling representation of **usf**-ZMOF displaying a **med** topology, $2[4^9{\cdot}6^2{\cdot}8^3] + [4^{10}{\cdot}6^4{\cdot}8^4]$.

DMA^+, and the ion-exchanged Li^+ and Mg^{2+} samples) on the H_2 sorption energetics and uptake is reported.[132]

Findings reveal that molecular hydrogen in ion-exchanged ZMOFs (Fig. 11) clearly demonstrates that the presence of an electrostatic field in the cavity is largely responsible for the observed improvement in the isosteric heats of adsorption in these compounds, by as much as 50%, relative to those in neutral MOFs. The extra-framework cations are fully coordinated by aqua ligands, and are not directly accessible to the H_2 molecules; thus, open-metal sites do not contribute to a dramatic increase in the overall binding energies. However, these results are promising and may be regarded as the first of several steps towards improving binding energies to values around 15–20 kJ mol^{-1}.

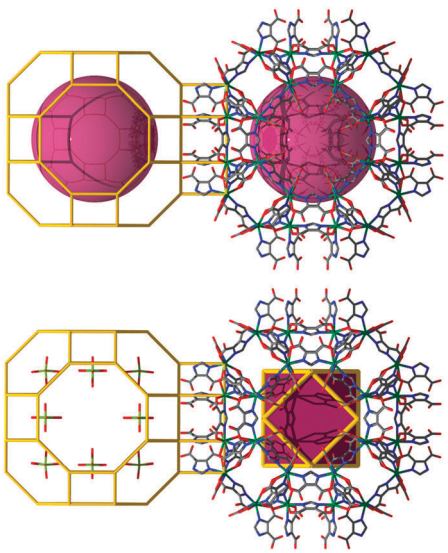

Fig. 11 Fragment of **rho**-ZMOF-1, where the interior size of the extra-large α-cavity is represented by a purple sphere (top), and fragment of the single-crystal structure of Mg-**rho**-ZMOF-1 showing the α-cages (gold) and the cubohemioctahedral arrangement (shown as a purple polyhedron) of the twelve $[Mg(H_2O)_6]^{2+}$ per cage (bottom).

ZMOFs offer great potential for reaching this goal by tuning the accessible extra-framework cations and/or introducing open-metal sites, along with a reduction in pore size and functionalization on the organic links.

At the same time, the large pores of ZMOFs are well-suited to adsorb not just metal ions, but also larger molecules, like cationic fluorophores for sensing-related applications, for example. The double eight-member ring (d8R) cages of In-HImDC **rho**-ZMOF-1 represent ~9 Å windows that allow access to the extra-large cavities, α-cages, with an internal diameter of 18.2 Å. The cationic fluorophore, protonated acridine orange (AO), is of the appropriate size, and can be diffused into the α-cage cavities, where the electrostatic interactions with the framework preclude further diffusion of cationic AO out of the cavities/pores, essentially anchoring the fluorophore (Fig. 12).[15] The extra-large dimensions allow for the diffusion of additional neutral guest molecules, and the anchored cationic AO is utilized to sense a variety of neutral molecules, such as methyl xanthines or DNA nucleoside bases.[15,88]

Adsorption of large molecules for sensor applications in In-HImDC **rho**-ZMOF-1 opens up the possibility of evaluating its extra-large cavities as hosts for large catalytically active molecules, and its effect on the enhancement of catalytic activity. In recent studies, the successful encapsulation of free base porphyrin $[H_2TMPyP][p\text{-tosyl}]^{4+}$ was probed, followed by post-synthetic metallation by various transition metal ions to produce a wide range of encapsulated metalloporphyrins (Fig. 13).[133] The catalytic activity assessment consists of cyclohexane oxidation, performed in the presence of Mn-TMPyP. After 24 h, based on the amount of oxidant present in the initial reaction mixture, a total yield (from cyclohexane to cyclohexanol/cyclohexanone) of 91.5% and a corresponding turn over number (TON) of 23.5 (catalyst loading of 3.8%) are noted, a noticeably higher yield compared to other systems of supported metalloporphyrins (*e.g.*, zeolites or mesoporous silicates).

More recently, the single-metal-ion-based MBB approach to design and synthesize a variety of ZMOFs has been successfully

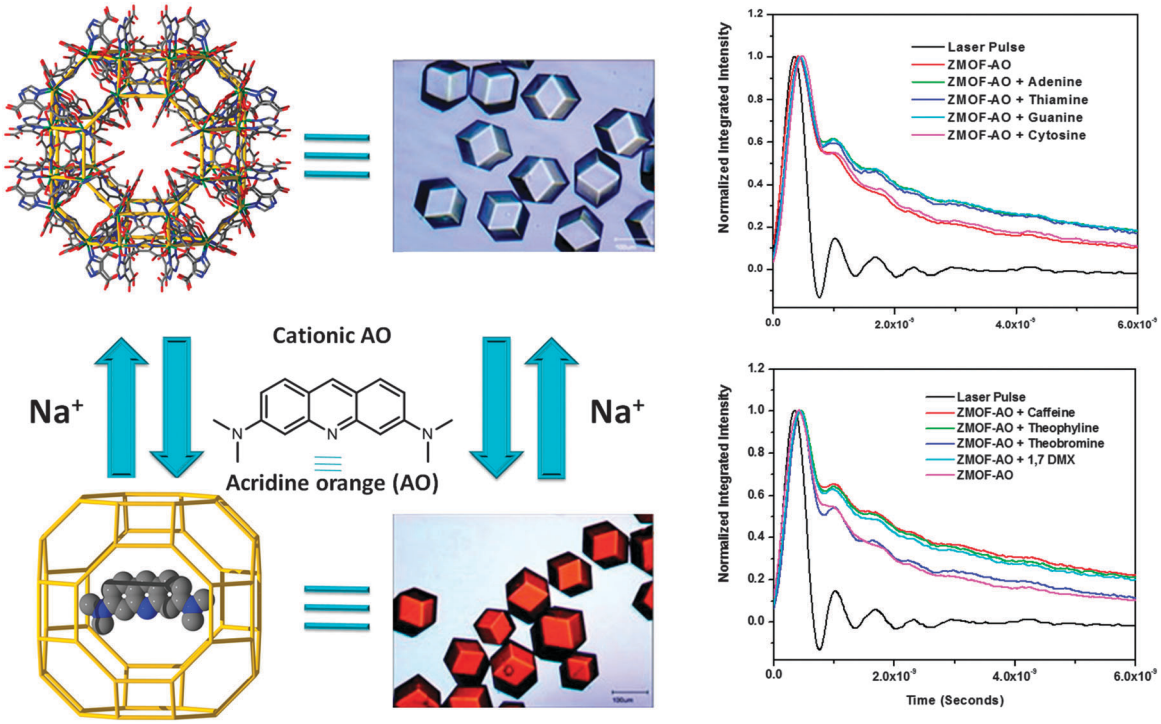

Fig. 12 Schematic and optical images of the **rho**-ZMOF-1 before (above) and after (bottom) cationic AO exchange. Fluorescence lifetime decay for cationic AO-**rho**-ZMOF-1 in the presence of various nucleoside bases and methyl xanthines (right).

supported by work conducted with other angular hetero-functional bis-chelating bridging ligands, namely pyrimidinecarboxylates.[87] Reaction between $In(NO_3)_3{\cdot}5H_2O$ and 4,6-pyrimidinedicarboxylate (4,6-PmDC) under hydro-solvothermal conditions yields another anionic **sod**-ZMOF, (Fig. 14 left), from $InN_4(O_2C{-})_4$ MBBs (InN_4 TBUs). Reaction between 2-cyanopyrimidine (where the 2-pyrimidinecarboxylate (2-PmC), was generated *in situ*) and $Cd(NO_3)_2{\cdot}4H_2O$, in the presence of piperazine (Pip) and under hydro-solvothermal conditions, produces another **rho**-ZMOF, (Fig. 14 right), from $CdN_4(O_2C{-})_4$ MBBs (CdN_4 TBUs).

The inherent properties of these ZMOFs allow for the evaluation of a breadth of properties. Full ion exchange in water based solutions at room temperature over short periods of time (less than 24 hours) was conducted on the anionic In-PmDC **sod**-ZMOF-2 (results confirmed by atomic absorption). The structural integrity is maintained as evidenced by PXRD analysis. Gas sorption (H_2, Ar, N_2) studies were also performed, evidencing accessible porosity with apparent Langmuir surface areas estimated to be 616 $m^2\ g^{-1}$ for In-PmDC **sod**-ZMOF-2, and considerably higher for Cd-PmC **rho**-ZMOF-2, 1168 $m^2\ g^{-1}$. The deliberate enhancement of the framework-hydrogen interactions is an ongoing challenge. In this context, an increase in the isosteric heat of adsorption was observed in anionic ZMOFs, due to the presence of high local charge density. These unique compounds are therefore suited to outline a functional platform for investigation of the effect of pore size and charge, as well as the effect of various extra-framework cations, upon the hydrogen isosteric heats of adsorption and uptakes.

Another advanced single-metal-ion-based strategy that may allow access to new, open ZMOFs involves the use of chelating carboxylate ligands (L), where, specifically, three-member rings are preferentially produced *in situ*. It has been theorized that this specific three-member ring building unit, which has the smallest possible ring size, can be utilized to create new topological types with low framework density, and is highly recommended in developing strategies for construction of new porous materials.

Along this route, Bu *et al.* reported the use of the MBB approach, with indium-based TBUs, to target new zeolitic MOFs built up from In_3L_3 three-member rings by using a mixed-ligand strategy. Indeed, mixed dicarboxylate linkers with 120° and 180° angles were employed with indium ions to generate a series of 3D crystalline porous materials (CPM) displaying zeolitic **npo** topology.[134] The structure of CPM-2-NH_2 consists of three crystallographically independent In^{3+} ions coordinated by four bidentate carboxylates (InO_8, to give $In(O_2C{-})_4$ TBU) from two bent dicarboxylate ligands (L) and two biphenyl dicarboxylate (bpdc) ligands (L′), giving rise to triangular (In_3L_3) groups acting as SBUs. Each SBU is connected to six neighboring SBUs through six linear ligands resulting in the formation of a 3D zeolitic **npo** framework (Fig. 15).

The MBB approach based on rigid and directional single-metal ion TBUs derived from heterochelating organic ligands, as well as chelating ligands, has been proven to be an effective and versatile strategy for the construction of ZMOFs. The resemblance to traditional zeolitic materials is outlined from a topological viewpoint, as well as in the anionic nature and synthesis (use of SDAs), and properties related to these materials. Furthermore, the superior ability of ZMOFs to fine-tune was proven, as the pore size, charge density, and surface areas were readily altered, leading to the development of a solid platform for relevant applications.[15,88,132,133]

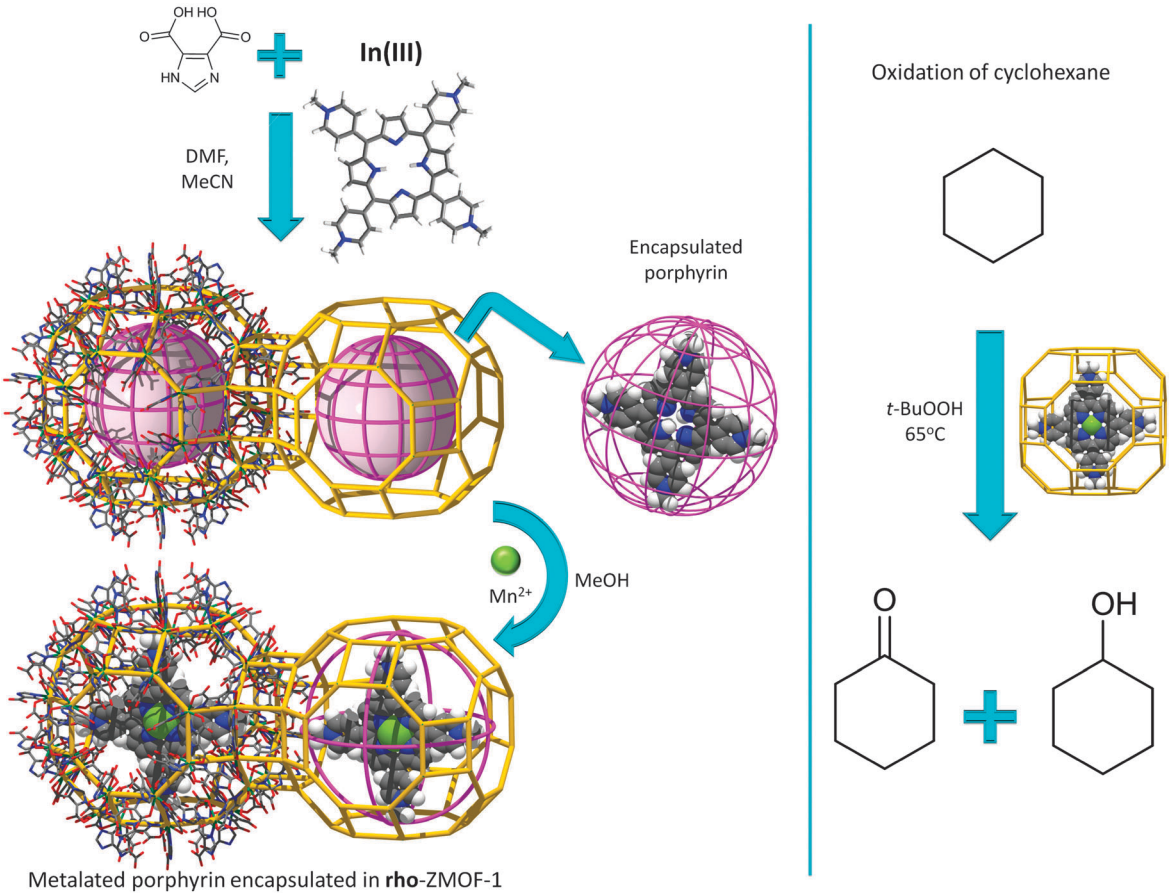

Fig. 13 Schematic representation of the encapsulation and metallation of the $[H_2TMPyP]^{4+}$ porphyrin ring enclosed in the **rho**-ZMOF-1 α-cage (left); the pink spherical cage schematically represents the average localization of the encapsulated porphyrin in the **rho**-ZMOF-1 α-cage. Catalytic activity from cyclohexane to cyclohexanol/cyclohexanone in the presence of the ZMOF-metalloporphyrin (right).

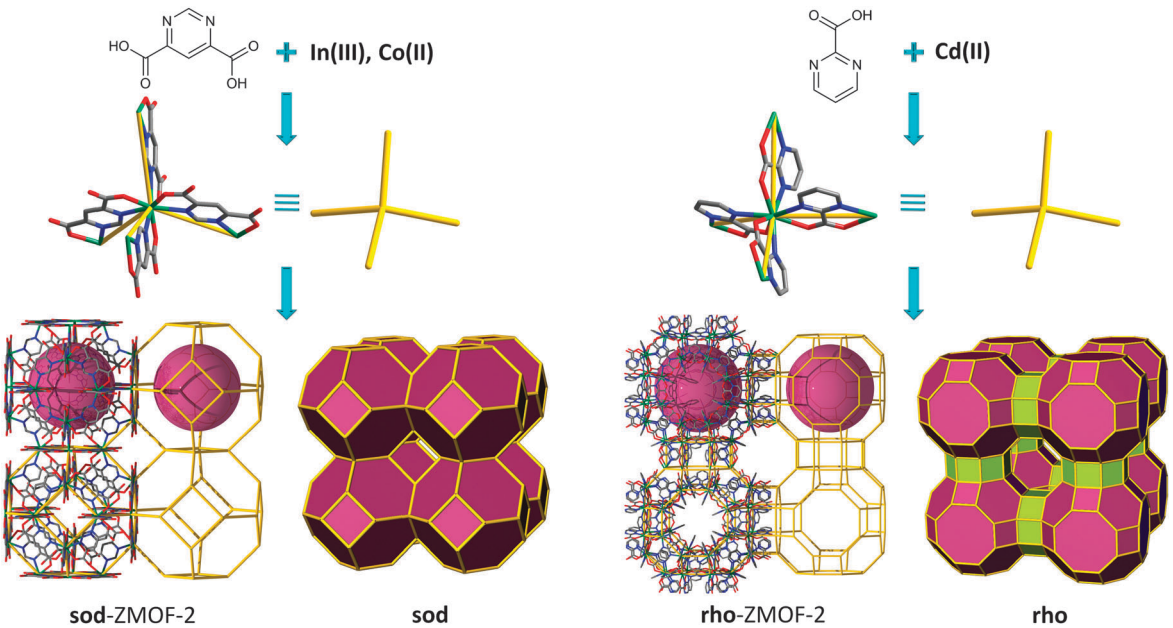

Fig. 14 Pyrimidinecarboxylate-based ZMOFs: **sod**-ZMOF-2 (left) and **rho**-ZMOF-2 (right).

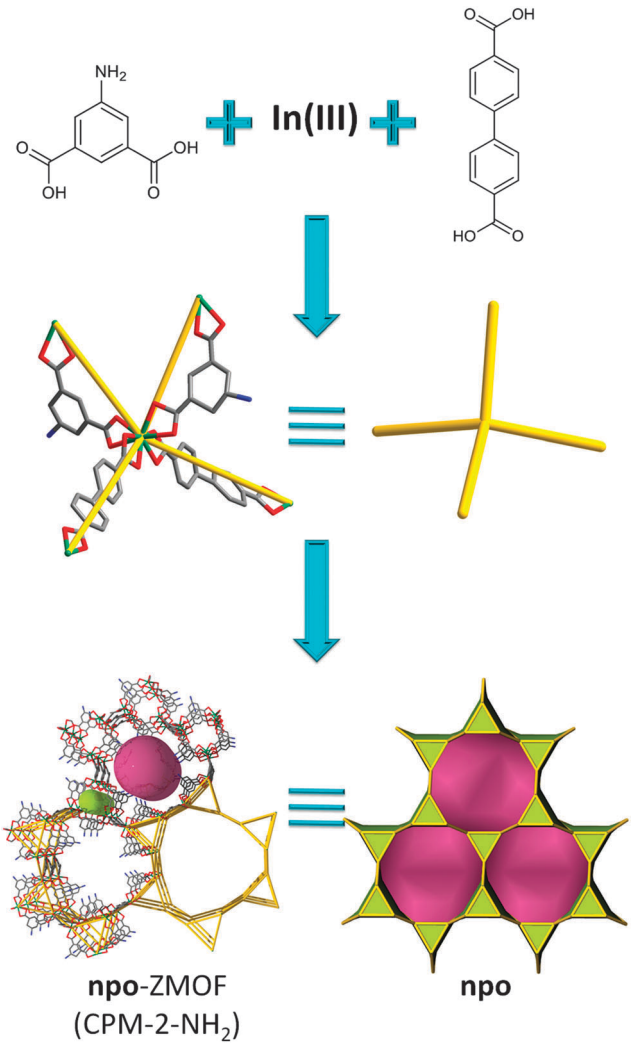

Fig. 15 **npo**-like framework based on mixed, bent and linear, dicarboxylate linkers; tiling and structural representation of **npo** topology with $[3^2{\cdot}6^3] + [6^3{\cdot}12^2]$.

4. ZMOFs derived from metal–organic cubes (MOCs)

An alternative route toward intended ZMOFs is probed by means of the introduction of a superior level of built-in information prior to the assembly process, beyond even single-metal-ion-based MBBs, a condition made possible by utilizing MOPs as supermolecular building blocks (SBBs), as previously demonstrated by our group,[135–138] among others.[139,140] Accordingly, a suitable approach to access ZMOFs is based on the assembly of metal–organic cubes (MOCs), which resemble d4R composite building units in inorganic zeolites. By utilizing the previously delineated single-metal-ion-based MBB approach, our group reported the synthesis of a metal–organic cube, MOC-1.[128] In this robust assembly, the ditopic heterofunctional imidazoledicarboxylate ligands represented the edges of the cubes, while the single-metal-ion MBBs occupied its vertices.

The unique structure of this MOC, among others, leads to peripheral functional groups/coordination sites, which offer the potential for external coordination to metal ions and/or hydrogen bonding. In this context, MOCs are equivalent to the d4R composite building units in zeolites, and hence could also be regarded as suitable SBBs to construct structures based on the connection of d4Rs. Specifically, these MOC-based SBBs are suitable for the targeted synthesis of non-default nets, such as some of the 8-connected edge-transitive nets (where the cube is the vertex figure of an 8-connected node, and edge-transitive refers to the fact that structures contain only one type of edge). Moreover, the augmentation of edge-transitive nets, such as **bcu**, **flu**, **scu** and **reo**, outlines a close relationship with some corresponding zeolite-like frameworks, namely, ACO, AST, ASV, and LTA.[129,141] The MOC SBBs can be linked to form extended frameworks in two different ways (as depicted in Fig. 16): (1) through linear connections, where nets based on zeolites ACO and LTA can be accessed or (2) cross-linked through additional 4-connected (tetrahedral) nodes, to result in materials with AST and ASV-like zeolitic topologies.

Indeed, reaction of $In(NO_3)_3{\cdot}5H_2O$ with 4,5-dicyanoimidazole (4,5-DCIm) in a DMF solution and in the presence of pip affords pale yellow homogeneous microcrystalline material with dodecahedron morphology, referred to as **aco**-ZMOF or MOC-2.[141] The cubes are linearly connected vertex-to-vertex *via* intermolecular hydrogen bonds, O–H···O, 2.786 Å. Each metal–organic cube concomitantly connects to eight neighbouring cubes through 24 hydrogen bonds, as the oxygen atoms pointing outward of each cube form three intermolecular hydrogen bonds with the corresponding oxygen atoms of the neighbouring cube. Consequently, the periodic arrangement of the discrete molecules results in an open framework that resembles the ACO zeolite topology (Fig. 16 left column).

The framework possesses accessible channels that can accommodate a sphere with a maximum diameter of 11.782 Å, considering the vdW radii of the nearest atoms, and an estimated Langmuir surface area of 1420 $m^2\ g^{-1}$. The material is exceptionally robust, in the context that the MOCs are solely sustained by hydrogen bonds, and stores up to 2.15% weight H_2 at 77 K and atmospheric pressures.[141]

In addition to the previous example, the solvothermal reaction of $Cd(NO_3)_2{\cdot}4H_2O$ and H_3ImDC, in the presence of Na^+ ions, gives rise to a material in which each cube is vertex-to-vertex linearly linked to eight other MOCs. In this assembly, half of the total number of vertices is connected through four sodium atoms, while the other four vertices are bridged by hydrogen bonded water molecules (Fig. 16 middle column).[129] The framework of MOC-4 possesses an overall **lta** topology, where the α-cage is based on 12 MOCs, while 6 other cubes give rise to the formation of the β-cage. The largest sphere that can fit into the cavities without interacting with the vdW surface of the framework has an approximate diameter of ~32 Å for the α-cage and ~8.5 Å for the β-cage.[129]

Examples of tetrahedrally connected MOCs were also achieved experimentally.[141] The reaction between $In(NO_3)_3{\cdot}5H_2O$ and 4,5-DCIm in an EtOH solution yields colourless polyhedral crystals. The discrete cubes are connected by ammonium cations, which are linking four MOCs in a tetrahedral arrangement through N–H···O hydrogen bonds to generate a structure

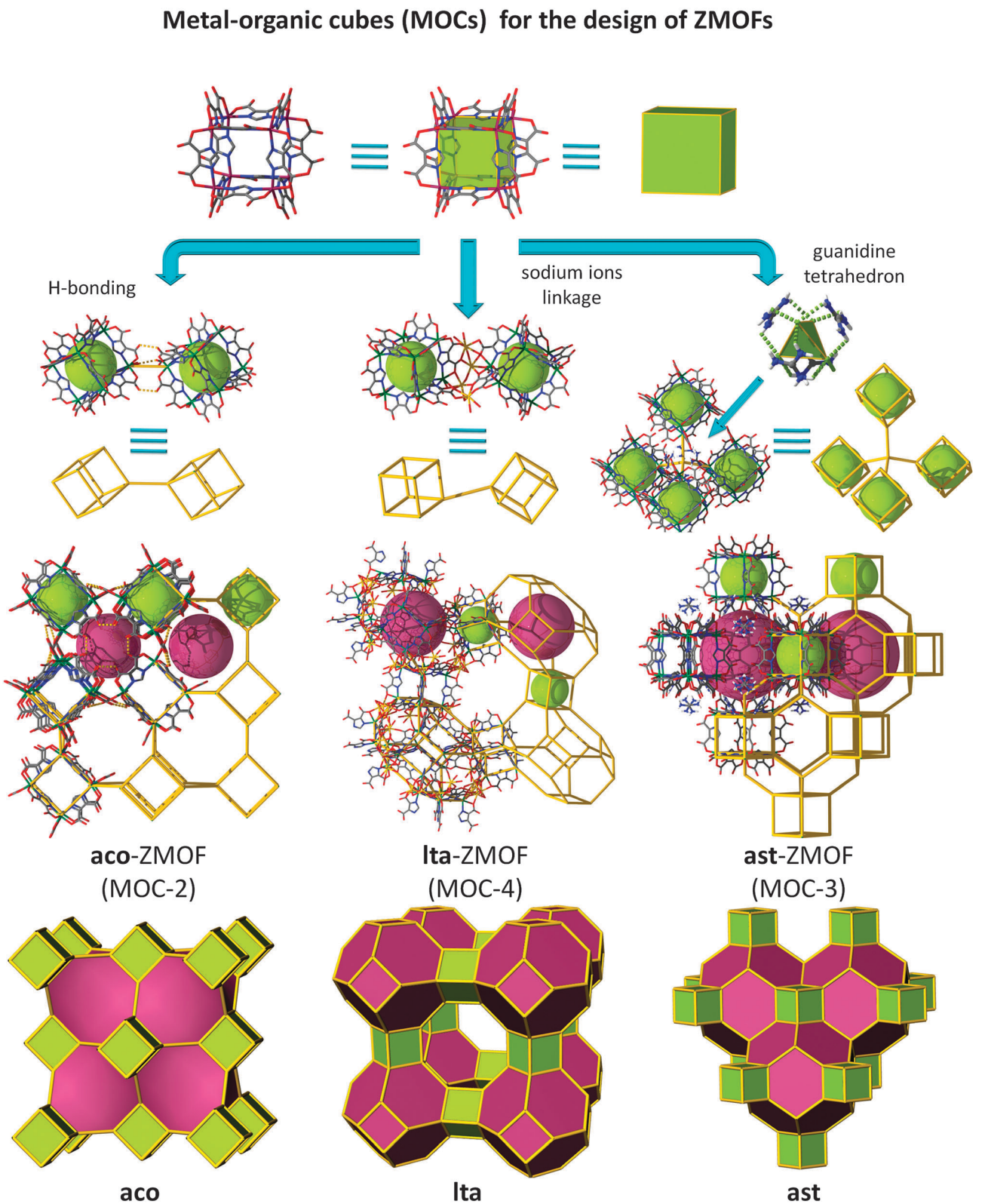

Fig. 16 Prototype scheme for MOC-to-ZMOF linkage: connectivity through (left and middle columns) linear linkers, resulting in **aco**-ZMOF and **lta**-ZMOF, as well as through tetrahedral nodes (right column), leading to the assembly of **ast**-ZMOF.

with the zeolite AST topology, **ast**-ZMOF-1, where the Langmuir surface area is estimated to be 456 $m^2\ g^{-1}$.

Another example based on **ast** topology, **ast**-ZMOF-2, is afforded by the reaction of H_3ImDC and $Zn(NO_3)_2{\cdot}6H_2O$ in a DMF–H_2O

solution, in the presence of excess zinc and guanidinium cations, (Fig. 16, right column).[129] Under these conditions, the MOCs are concomitantly connected through their edges and vertices to zinc and guanidinium ions, respectively, and further extend to twelve adjacent MOCs to yield yet another material with a zeolitic topology and features.

More recently, a systematic investigation using 2,2′-(1*H*-imidazole-4,5-diyl)di-1,4,5,6-tetrahydropyrimidine and different M^{2+} metal ions was conducted to elucidate the effect of different parameters, such as the nature of metal ions, counterions, solvent systems, solution pH, and temperature, on the nature of isolated MOC products.[130] It was demonstrated that the formation of a given targeted MBB requires the careful choice of reaction conditions, *i.e.* reactant concentration, temperature, solvent mixture, metal ion, counterion, and pH. A properly chosen solvent system should promote desired ligand-to-metal coordination, as well as facilitate nucleation and crystallization. Counter-ions with limited interference to ligand coordination are vital for the metal–ligand directed assembly of the desired MBB necessary for the formation of a given MOF (or ZMOF).[130]

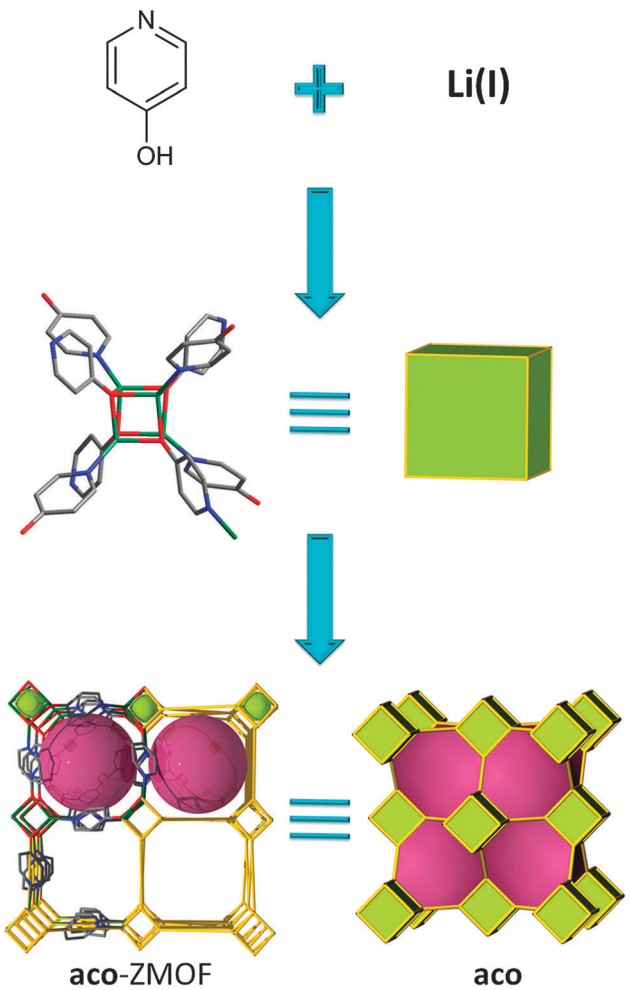

Fig. 17 Schematic illustration of the self-assembly from inorganic and organic species to 3-periodic MOF having the **aco** topology.

In all the MOC-based ZMOFs presented previously, the MOCs are built up from eight metals connected *via* eight ligands leading to an 8-connected SBU. However, it is also possible to target 8-connected MOCs constructed with only four metals and eight ligands. This strategy, reported by Feng *et al.*, has afforded a lithium-cubane-based MOF by using a ditopic ligand, 4-pyridinol (Fig. 17).[142] The structure can be regarded as a 3-periodic framework constructed by interconnecting $Li_4(OPy)_4$ cubane clusters through Li–N bonding. The resulting topology can be understood as a **bcu** net. It is worth mentioning that, since all lithium and oxygen atoms are tetrahedrally coordinated, the resulting framework can be interpreted as an ACO topology.

In summary, this approach has proven to be pertinent to the construction of zeolite-like materials. The strategy conveys a superior route towards novel ZMOFs, outlining a hierarchical pathway initiated from single-metal ions with anticipated coordination geometries, and predesigned to act as rigid and directional vertices, into MOCs that can be utilized as d4Rs, to ultimately result into intended zeolitic frameworks, ZMOFs.

5. ZMOFs built from supertetrahedral (ST) building blocks

Metal–carboxylate clusters generated *in situ* represent MBBs commonly employed to target MOFs, since they possess metal–oxygen coordination bonds that result in the generation of rigid nodes with fixed geometry. Accordingly, they aid the formation of robust (and possibly, permanently porous) 3-periodic frameworks, as well as hold potential for open (or coordinatively unsaturated) metal sites that are of interest for various applications. Various organic linkers can be employed to connect such clusters that ultimately can result in solid-state materials with pore sizes that may go beyond the microporous regime, which is characteristic of the majority of MOFs.[143,144]

Metal–carboxylate clusters can also be utilized as a possible pathway to tetrahedral-based zeolitic MOFs; ZMOFs can be attained through access to tetrahedral-like building blocks based on metal–carboxylate clusters, which, in combination with linker connectivity, comprise the necessary requirements to be translated into supertetrahedral (ST) building units. The ST building block can be viewed as the enlarged version of a simple tetrahedral vertex, having, as a final outcome, a material with analogous topology, only on an expanded scale, albeit a different method from the aforementioned edge-expansion.

In this context, investigations carried out by Férey and co-workers resulted in two porous solid-state materials, MIL-100[72] and MIL-101,[73] that outline the decorated and augmented **mtn** zeolite topology. The group's approach is focused on rendering rigid carboxylate-based metal clusters that maintain, unaltered, their pre-designed function throughout the assembly process. Specifically, they utilized building blocks derived from trimeric units constructed from three metal octahedra meeting at a vertex (V), μ_3-O (of the type $M_3O(O_2CR)_6L_3$), to generate an overall ST building unit, where, in MIL-100, the carboxylates come from trimesic acid, or 1,3,5-benzenetricarboxylate (1,3,5-BTC), ligand (L),

which lies on the four faces of the ST ($(M_3O)_4L_4$ or V_4L_4), while the trimers occupy its vertices. By linking the corners of the STs, the material possesses decorated and augmented **mtn** topology (by definition, augmentation being referred to as the replacement of each vertex of an N-connected net by N-vertices, *i.e.*, in this case, a tetrahedron by a ST). The structure exhibits two different types of cages: the smaller cage (~25 Å in diameter) consists of 20 ST, while the larger cages are built from 28 ST (~29 Å in diameter), highlighting an apparent Langmuir surface area of 3100 $m^2\ g^{-1}$.

Soon after this discovery, Férey *et al.* reported the synthesis of MIL-101, a material also based on M^{3+} trimer inorganic clusters (the same as in MIL-100), but in the presence of a different linker, namely 1,4-benzenedicarboxylic acid (1,4-BDC). Similar to MIL-100, a ST is generated by the arrangement of the trimers on its vertices; however, in this instance, the linker represents the edge of the ST ($(M_3O)_4L_6$ V_4L_6), bridging the vertices in the intended tetrahedral arrangement (Fig. 18). The two types of cages are once again comprised of 20 ST (~29 Å in diameter) for the small cage and 28 ST for the large cage (~34 Å in diameter), with an exploitable outstanding estimated Langmuir surface area of 5900 $m^2\ g^{-1}$.[73] Very recently, a series of isoreticular analogues of MIL-100 and MIL-101 showing an exceptional pore size, of up to 68 Å, have been synthesized.[145,146]

Gas (hydrogen, CO_2, and CH_4) sorption capabilities were evaluated on both MIL-100 and MIL-101.[117,147] In the context of reducing the effects of greenhouse gases, it was shown that both compounds exhibit remarkable results in storing large amounts of CO_2 and CH_4 at relatively high pressures (>5 MPa)

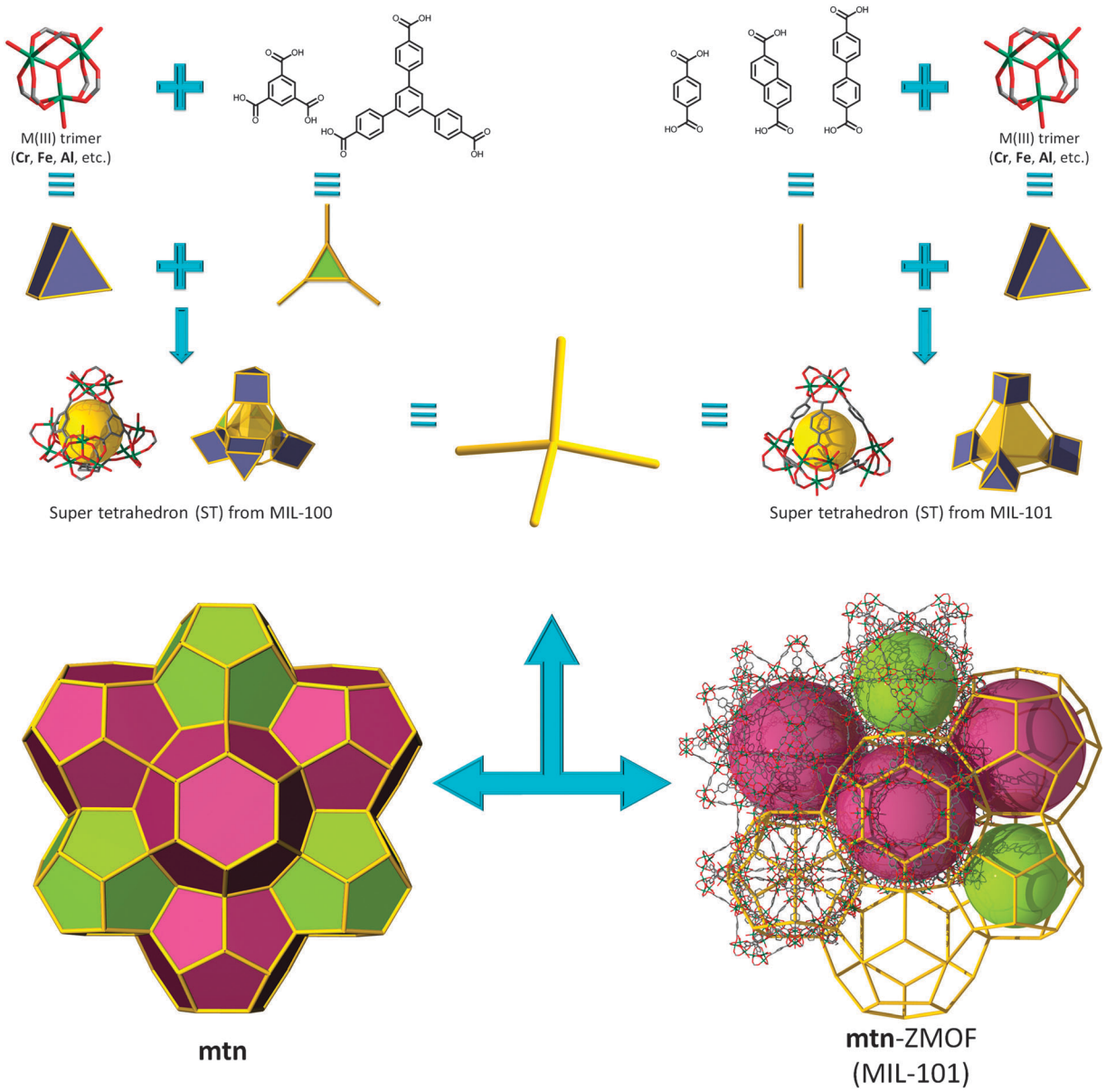

Fig. 18 Supertetrahedron (ST) building units based on M^{III} trimers and triangular (MIL-100's, left) or linear (MIL-101's, right) leading to the assembly of gigantic **mtn**-ZMOFs.

and ambient temperatures. Specifically, at 6 MPa and 300 K, MIL-100 adsorbs 9.5 mmol g^{-1} CH_4 and 18 mmol g^{-1} of CO_2 at 5 MPa and 300 K. As expected, MIL-101 performs superior to MIL-100 adsorbing 13.6 mmol g^{-1} methane at 6 MPa and 300 K and 40 mmol g^{-1} of CO_2 at 5 MPa and 300 K. Further evaluations illustrate the potential for drug delivery applications. Studies confirmed the uptake and controlled release of ibuprofen (IBU), among others,[148] from the extra-large pores of MIL-100 (apertures of 4.8 Å and 8.6 Å) and MIL-101 (apertures of 12 Å and 16 Å), with 0.347 g IBU per gram of dehydrated MIL-100 and 1.376 g of IBU per gram of dehydrated MIL-101.

Another example pertinent to this approach was reported by Kim *et al.*[74] where the framework is built from truncated ST formed by four terbium metal ions that constitute its vertices. The arrangement of these units, aided by the linkage provided by the triazine-1,3,5-tribenzoic acid (H_3TATB), contributes to the generation of a mesoporous material also with **mtn** zeolite topology. The two mesoporous cages are denoted S (20 truncated STs formed by twelve 5-MR, 39.1 Å) and L (28 truncated STs, with twelve 5-MR and four 6-MR windows, 47.1 Å), and generate a Langmuir surface area of 3855 m^2 g^{-1}, after sample activation at 160 °C. High-pressure CO_2 gas sorption studies confirmed considerable amounts of gas stored under these conditions (18 mmol g^{-1} at *ca.* 45 bar and ambient temperature).

A variant strategy towards constructing hybrid materials with zeolitic topologies derived from ST-based building blocks was undertaken by a computational driven approach. The concept involves organic linkers (such as 1,4-benzenedicarboxylate and imidazole), where the tetrahedral single-metal ion center is replaced by Zn capped ε-type Keggin polyoxometalates (POMs), targeting the assembly of zeolitic polyoxometalate-based metal–organic frameworks (Z-POMOFs).[149,150] Theoretical studies validate this strategy by predicting a series of structures with zeolitic topologies based on such "exotic" building blocks. Experimentally, only two examples were accessed using this method to date; however, none possesses zeolitic features. In one instance, the default diamondoid net is reported,[150] while a subsequent example exhibits a layered structure.[149] Once again, this approach outlines the difficulty associated with the synthesis of highly porous zeolite-like nets. At the same time, it stresses the importance of concrete design concepts mediated by modelling approaches.

6. ZMOFs constructed *via* organic tetrahedral nodes

The final method to construct ZMOFs that we will describe is based on a so-called "inverted" approach, in which the organic molecules act as tetrahedral nodes. This concept involves metal ions with various coordination numbers required to act as the angular ditopic linkers, while auxiliary, weakly-coordinating ligands satisfy the remaining coordination sites of the metals. Ultimately, the organic TBUs have to be positioned at suitable angles (average of ~144°) in order to facilitate structures with zeolite-like features.

The four nitrogen atoms in hexamethylenetetramine (HMTA), situated in a tetrahedral arrangement, qualify this molecule as a potential organic tetrahedral node. From the work of Qiu *et al.* comes an example of a zeotype material with **mtn** topology (Fig. 19), constructed from the bridging of HMTA ligands *via* the 2-connected trigonal bipyramidal Cd(II) cations.[75]

The resulting cationic 3-periodic net (where the charge balance is ensured by chloride anions) is constructed from two types of cages: the large cage consists of four 6-MR, 12.3 Å × 13.1 Å, and twelve 5-MR, 10.4 Å × 10.4 Å in diameter, while the smaller cage consists of twelve 5-MR. The overall volume of the unit cell is 117 225 $Å^3$, as compared to 7920 $Å^3$ of the corresponding inorganic analogue. Anionic exchange of Cl^- with SCN^- was carried out, probing favourable retention of the framework profile upon such treatment.

More recently, the design and synthesis of novel tetracarboxylic acid ligands based on isophthalic moieties have allowed Xu *et al.* to construct a new ZMOF.[151] The so-called 4 + 4 strategy has been employed using 5-(bis(4-carboxybenzyl)amino)isophthalic acid, where the central N atom plays a crucial role in the conformation, as well as the indium cation that is well-known to coordinate to four carboxylate groups in a bidentate fashion, $In(O_2CR)_4$ (as highlighted previously in this *review*). The combination of these two kinds of tetrahedral nodes, $In(O_2CR)_4$ and the ligand, respectively, leads to the formation of an overall 3D anionic framework

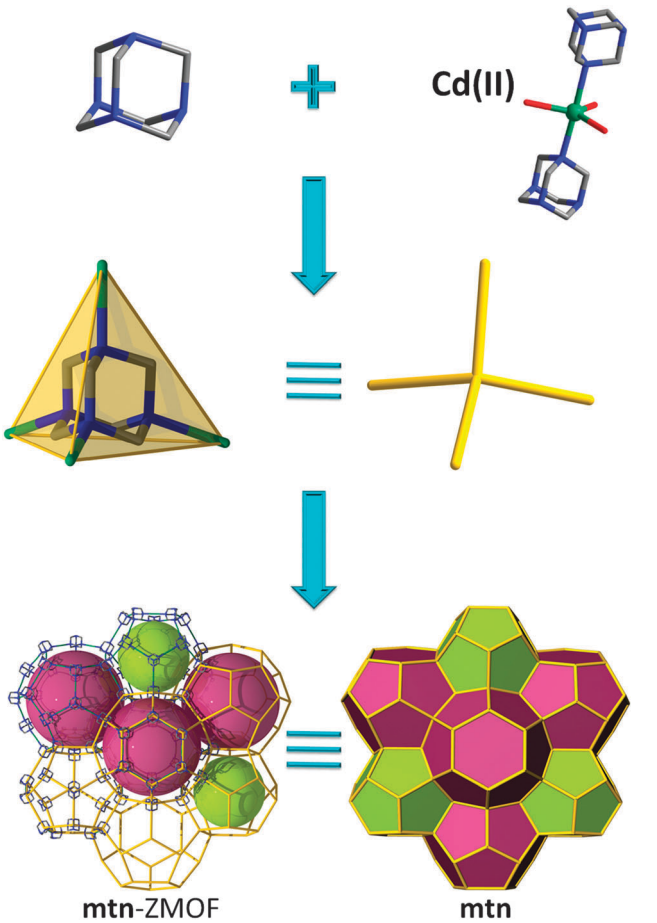

Fig. 19 **mtn**-like framework based on organic (HMTA) tetrahedral nodes; structural and tiling representation of **mtn** topology with 2[5^{12}] + [5^{12}·6^4] tiles.

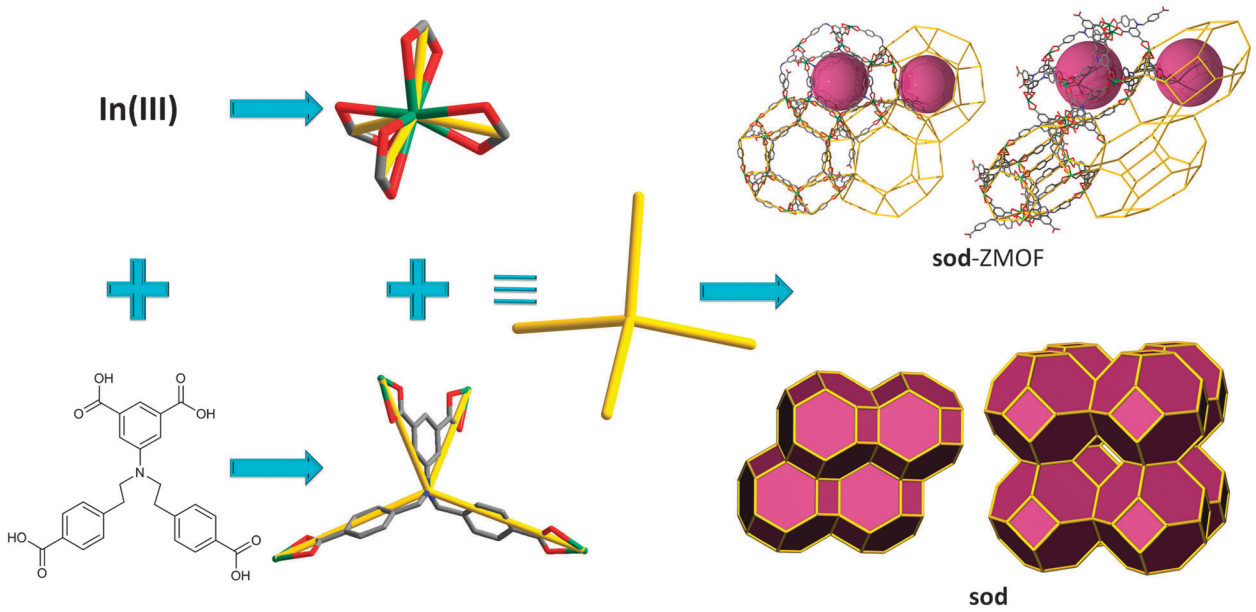

Fig. 20 Association of a 5-(bis(4-carboxybenzyl)amino)isophthalic acid as a tetrahedral node (bottom) with the $In(O_2CR)_4$ unit acting as a tetrahedral node (top), giving rise to a MOF based on **sod** topology.

adopting a **sod** topology (Fig. 20). The structure delimits sodalite cages with dimensions of 26 × 26 × 8.2 Å in which are localized DMA^+ cations that ensure the overall charge balance of the structure.

7. Summary and outlook

In the continuous endeavour to produce functional materials for targeted applications, MOFs are becoming strong candidates for meeting current societal and technological needs. In this *review*, the focus was placed on identifying possible strategies and relevant examples of MOFs that possess periodic intra-framework organic functionality and zeolite-like topologies and properties. The portrayed examples demonstrate that complex structures, based on non-default nets, such as zeolite-like MOFs (ZMOFs), not only can be discovered serendipitously or through high throughput methods, but also, more importantly, can be designed and assembled by the rational choice of rigid and directional building blocks containing the required hierarchical information. The presented strategies offer great potential to access complex structures that are not readily constructed from the conventional assembly of simple building blocks, aiding the advancement in the design and synthesis of functional materials.

Solid-state materials with large and extra-large cavities, such as ZMOFs, allow for a multitude of diverse studies that complement areas where traditional zeolite materials encounter limited tunability. *Ipso facto*, innovative functions are arising from the specificity associated with their porous nature. Most concerted efforts highlight gas sorption/separation studies (*e.g.*, hydrogen storage as a clean energy source for mobile applications, and selective storage and separation of greenhouse gases (CO_2 and CH_4)). The uptake and controlled release of drugs gear their functions towards other sectors, as well. Recent results demonstrate the ability of anionic ZMOFs to serve as (host–guest)–guest sensors, where the ZMOF portrays a periodic porous platform for fluorescent cations that act as the sensors,[15,88,152] as well as supporting catalytic activity mediated by the encapsulation and metallation of metalloporphyrins.[133]

Nonetheless, as the ability to engineer functional porous solid-state materials has been greatly developed through rational design strategies, the actual synthetic process still requires substantial efforts. Ultimately, the main goal regards the ability to precisely construct the desired material for the intended purpose; in perspective, the propensity for vast advancements in materials chemistry based on zeolite-like MOFs is indubitably highly valuable and holds great promise for novel materials and applications.

Acknowledgements

This work was supported by the King Abdullah University of Science and Technology (KAUST).

Notes and references

1 M. Eddaoudi and J. F. Eubank, *Organic Nanostructures*, Wiley-VCH Verlag GmbH & Co. KGaA, 2008, pp. 251–274.
2 O. M. Yaghi, H. L. Li, C. Davis, D. Richardson and T. L. Groy, *Acc. Chem. Res.*, 1998, **31**, 474–484.
3 S. L. James, *Chem. Soc. Rev.*, 2003, **32**, 276–288.
4 H. K. Chae, D. Y. Siberio-Perez, J. Kim, Y. Go, M. Eddaoudi, A. J. Matzger, M. O'Keeffe and O. M. Yaghi, *Nature*, 2004, **427**, 523–527.
5 S. Kitagawa, R. Kitaura and S.-i. Noro, *Angew. Chem., Int. Ed.*, 2004, **43**, 2334–2375.

6 B. Moulton and M. J. Zaworotko, *Chem. Rev.*, 2001, **101**, 1629–1658.
7 O. Kahn, *Acc. Chem. Res.*, 2000, **33**, 647–657.
8 C. N. R. Rao, S. Natarajan and R. Vaidhyanathan, *Angew. Chem., Int. Ed.*, 2004, **43**, 1466–1496.
9 O. R. Evans and W. Lin, *Acc. Chem. Res.*, 2002, **35**, 511–522.
10 C. Janiak, *Dalton Trans.*, 2003, 2781–2804.
11 G. Férey, *Chem. Soc. Rev.*, 2008, **37**, 191–214.
12 M. Kondo, T. Okubo, A. Asami, S.-i. Noro, T. Yoshitomi, S. Kitagawa, T. Ishii, H. Matsuzaka and K. Seki, *Angew. Chem., Int. Ed.*, 1999, **38**, 140–143.
13 M. Eddaoudi, J. Kim, N. L. Rosi, D. T. Vodak, J. B. Wachter, M. O'Keeffe and O. M. Yaghi, *Science*, 2002, **295**, 469–472.
14 M. Dincă and J. R. Long, *Angew. Chem., Int. Ed.*, 2008, **47**, 6766–6779.
15 Y. Liu, V. C. Kravtsov, R. Larsen and M. Eddaoudi, *Chem. Commun.*, 2006, 1488–1490.
16 B. F. Hoskins and R. Robson, *J. Am. Chem. Soc.*, 1990, **112**, 1546–1554.
17 A. Stein, S. W. Keller and T. E. Mallouk, *Science*, 1993, **259**, 1558–1564.
18 G. Férey, *J. Solid State Chem.*, 2000, **152**, 37–48.
19 M. Eddaoudi, J. Kim, D. T. Vodak, A. Sudik, J. B. Wachter, M. O'Keeffe and O. M. Yaghi, *Proc. Natl. Acad. Sci. U. S. A.*, 2002, **99**, 4900–4904.
20 M. Eddaoudi, D. B. Moler, H. L. Li, B. L. Chen, T. M. Reineke, M. O'Keeffe and O. M. Yaghi, *Acc. Chem. Res.*, 2001, **34**, 319–330.
21 A. K. Cheetham, G. Férey and T. Loiseau, *Angew. Chem., Int. Ed.*, 1999, **38**, 3268–3292.
22 O. M. Yaghi, M. O'Keeffe, N. W. Ockwig, H. K. Chae, M. Eddaoudi and J. Kim, *Nature*, 2003, **423**, 705–714.
23 Y. Liu, J. F. Eubank, A. J. Cairns, J. Eckert, V. C. Kravtsov, R. Luebke and M. Eddaoudi, *Angew. Chem., Int. Ed.*, 2007, **46**, 3278–3283.
24 M. E. Davis, *Nature*, 2002, **417**, 813–821.
25 X. Yang, *Gongye Cuihua*, 2003, **11**, 19–24.
26 I. E. Maxwell and W. H. J. Stork, in *Studies in Surface Science and Catalysis*, ed. H. v. Bekkum, E. M. Flanigen, P. A. Jacobs and J. C. Jansen, Elsevier, 2001, vol. 137, pp. 747–819.
27 A. Corma, in *Zeolite Microporous Solids: Synthesis, Structure, and Reactivity*, ed. E. Derouane, F. Lemos, C. Naccache and F. Ribeiro, Springer, Netherlands, 1992, vol. 352, pp. 373–436.
28 R. Gläser and J. Weitkamp, in *Basic Principles in Applied Catalysis*, ed. M. Baerns, Springer, Berlin, Heidelberg, 2004, vol. 75, pp. 159–212.
29 K. Hagiwara, T. Ebihara, N. Urasato, S. Ozawa and S. Nakata, *Appl. Catal., A*, 2003, **249**, 213–228.
30 R. P. Claridge, N. L. Lancaster, R. W. Millar, R. B. Moodie and J. P. B. Sandall, *J. Chem. Soc., Perkin Trans. 2*, 2001, 197–200.
31 G. Hourdin, A. Germain, C. Moreau and F. Fajula, *Catal. Lett.*, 2000, **69**, 241–244.
32 S. M. Kuznicki, V. A. Bell, T. W. Langner and J. S. Curran, *US Pat.*, US 20020074293, 2002.
33 S. M. Kuznicki, T. W. Langner and J. S. Curran, *US Pat.*, US 20020077245, 2002.
34 R. Le Van Mao, *Can. Pat.*, CA 2125314, 1995.
35 R. Le Van Mao, N. T. Vu, S. Xiao and A. Ramsaran, *J. Mater. Chem.*, 1994, **4**, 1143–1147.
36 D. W. Breck, *Zeolites molecular sieves*, Wiley-Interscience, New York, 1974, pp. 725–755.
37 *Molecular sieve zeolite. I. Advances in Chemistry Series No. 101*, ed. R. F. Gould, American Chemical Society, Washington, DC, 1971.
38 C. Baerlocher and L.B. McCusker, *Database of Zeolite Structures*, 2008, http://www.iza-structure.org/databases/.
39 M. O'Keeffe, M. Eddaoudi, H. Li, T. Reineke and O. M. Yaghi, *J. Solid State Chem.*, 2000, **152**, 3–20.
40 D.-X. Xue, A. J. Cairns, Y. Belmabkhout, Ł. Wojtas, Y. Liu, M. H. Alkordi and M. Eddaoudi, *J. Am. Chem. Soc.*, 2013, **135**, 7660–7667.
41 M. Li, D. Li, M. O'Keeffe and O. M. Yaghi, *Chem. Rev.*, 2013, **114**, 1343–1370.
42 H. Furukawa, K. E. Cordova, M. O'Keeffe and O. M. Yaghi, *Science*, 2013, 341.
43 N. W. Ockwig, O. Delgado-Friedrichs, M. O'Keeffe and O. M. Yaghi, *Acc. Chem. Res.*, 2005, **38**, 176–182.
44 M. O'Keeffe, M. A. Peskov, S. J. Ramsden and O. M. Yaghi, *Acc. Chem. Res.*, 2008, **41**, 1782–1789.
45 M. J. Zaworotko, *Chem. Soc. Rev.*, 1994, **23**, 283–288.
46 D. Armentano, G. De Munno, F. Lloret and M. Julve, *Inorg. Chem.*, 1999, **38**, 3744–3747.
47 R. Banerjee, A. Phan, B. Wang, C. Knobler, H. Furukawa, M. O'Keeffe and O. M. Yaghi, *Science*, 2008, **319**, 939–943.
48 X.-C. Huang, Y.-Y. Lin, J.-P. Zhang and X.-M. Chen, *Angew. Chem., Int. Ed.*, 2006, **45**, 1557–1559.
49 K. S. Park, Z. Ni, A. P. Côté, J. Y. Choi, R. Huang, F. J. Uribe-Romo, H. K. Chae, M. O'Keeffe and O. M. Yaghi, *Proc. Natl. Acad. Sci. U. S. A.*, 2006, **103**, 10186–10191.
50 W. R. Gemmill, M. D. Smith and B. A. Reisner, *J. Solid State Chem.*, 2005, **178**, 2658–2662.
51 M. R. Udupa and B. Krebs, *Inorg. Chim. Acta*, 1980, **42**, 37–41.
52 S. J. Rettig, A. Storr, D. A. Summers, R. C. Thompson and J. Trotter, *Can. J. Chem.*, 1999, **77**, 425–433.
53 Y.-Q. Tian, Z.-X. Chen, L.-H. Weng, H.-B. Guo, S. Gao and D. Y. Zhao, *Inorg. Chem.*, 2004, **43**, 4631–4635.
54 N. Stock, K. Karaghiosoff and T. Bein, *Z. Anorg. Allg. Chem.*, 2004, **630**, 2535–2540.
55 B. J. Prince and M. M. Turnbull, *J. Coord. Chem.*, 1997, **41**, 339–345.
56 S. Drumel, P. Janvier, D. Deniaud and B. Bujoli, *J. Chem. Soc., Chem. Commun.*, 1995, 1051–1052.
57 K.-M. Park, M. Hashimoto, T. Kitazawa and T. Iwamoto, *Chem. Lett.*, 1990, 1701–1704.
58 K.-M. Park and T. Iwamoto, *J. Inclusion Phenom. Macrocyclic Chem.*, 1991, **11**, 397–403.
59 L. A. Zasurskaya, I. N. Polyakova, A. L. Poznyak, T. N. Polynova and V. S. Sergienko, *Crystallogr. Rep.*, 2001, **46**, 377–382.
60 W.-T. Wong and C.-M. Che, *Acta Crystallogr., Sect. C: Cryst. Struct. Commun.*, 1994, **50**, 1407–1409.
61 H. Yuge and T. Iwamoto, *J. Inclusion Phenom. Macrocyclic Chem.*, 1992, **14**, 217–235.

62 X. Shi, G. Zhu, S. Qiu, K. Huang, J. Yu and R. Xu, *Angew. Chem., Int. Ed.*, 2004, **43**, 6482–6485.
63 Y.-Q. Tian, Y.-M. Zhao, Z.-X. Chen, G.-N. Zhang, L.-H. Weng and D.-Y. Zhao, *Chem. – Eur. J.*, 2007, **13**, 4146–4154.
64 S. Drumel, P. Janvier, P. Barboux, M. Bujoli-Doeuff and B. Bujoli, *Inorg. Chem.*, 1995, **34**, 148–156.
65 S.-I. Nishikiori and T. Iwamoto, *J. Inclusion Phenom.*, 1985, **3**, 283–295.
66 Q.-F. Zhang, W.-H. Leung, Q.-Z. Xin and H.-K. Fun, *Inorg. Chem.*, 2000, **39**, 417–426.
67 C. Zhang, Y. Song, Y. Xu, H. Fun, G. Fang, Y. Wang and X. Xin, *J. Chem. Soc., Dalton Trans.*, 2000, 2823–2829.
68 K. Tokoro, M. Ebihara and T. Kawamura, *Acta Crystallogr., Sect. C: Cryst. Struct. Commun.*, 1995, **51**, 2010–2013.
69 R. Vaidhyanathan, S. Natarajan and C. N. R. Rao, *Cryst. Growth Des.*, 2002, **3**, 47–51.
70 Y. Xu, L.-B. Nie, D. Zhu, Y. Song, G.-P. Zhou and W.-S. You, *Cryst. Growth Des.*, 2007, **7**, 925–929.
71 H. Hayashi, A. P. Côté, H. Furukawa, M. O'Keeffe and O. M. Yaghi, *Nat. Mater.*, 2007, **6**, 501–506.
72 G. Férey, C. Serre, C. Mellot-Draznieks, F. Millange, S. Surblé, J. Dutour and I. Margiolaki, *Angew. Chem., Int. Ed.*, 2004, **43**, 6296–6301.
73 G. Férey, C. Mellot-Draznieks, C. Serre, F. Millange, J. Dutour, S. Surblé and I. Margiolaki, *Science*, 2005, **309**, 2040–2042.
74 Y. K. Park, S. B. Choi, H. Kim, K. Kim, B.-H. Won, K. Choi, J.-S. Choi, W.-S. Ahn, N. Won, S. Kim, D. H. Jung, S.-H. Choi, G.-H. Kim, S.-S. Cha, Y. H. Jhon, J. K. Yang and J. Kim, *Angew. Chem., Int. Ed.*, 2007, **46**, 8230–8233.
75 Q. Fang, G. Zhu, M. Xue, J. Sun, Y. Wei, S. Qiu and R. Xu, *Angew. Chem., Int. Ed.*, 2005, **44**, 3845–3848.
76 M. L. Post and J. Trotter, *J. Chem. Soc., Dalton Trans.*, 1974, 1922–1925.
77 H. M. Dawes, J. M. Waters and T. Neil Waters, *Inorg. Chim. Acta*, 1982, **66**, 29–36.
78 N. Masciocchi, S. Bruni, E. Cariati, F. Cariati, S. Galli and A. Sironi, *Inorg. Chem.*, 2001, **40**, 5897–5905.
79 L. C. Tabares, J. A. R. Navarro and J. M. Salas, *J. Am. Chem. Soc.*, 2001, **123**, 383–387.
80 P. Naumov, M. Ristova, B. Soptrajanov, M.-J. Kim, H.-J. Lee and S. W. Ng, *Acta Crystallogr., Sect. E: Struct. Rep. Online*, 2001, **57**, m14–m16.
81 B. F. Abrahams, M. G. Haywood, R. Robson and D. A. Slizys, *Angew. Chem., Int. Ed.*, 2003, **42**, 1112–1115.
82 X. Huang, J. Zhang and X. Chen, *Chin. Sci. Bull.*, 2003, **48**, 1531–1534.
83 E. Barea, J. A. R. Navarro, J. M. Salas, N. Masciocchi, S. Galli and A. Sironi, *Polyhedron*, 2003, **22**, 3051–3057.
84 P. V. Solntsev, J. Sieler, A. N. Chernega, J. A. K. Howard, T. Gelbrich and K. V. Domasevitch, *Dalton Trans.*, 2004, 695–696.
85 E. Barea, J. A. R. Navarro, J. M. Salas, N. Masciocchi, S. Galli and A. Sironi, *J. Am. Chem. Soc.*, 2004, **126**, 3014–3015.
86 B. F. Abrahams, A. Hawley, M. G. Haywood, T. A. Hudson, R. Robson and D. A. Slizys, *J. Am. Chem. Soc.*, 2004, **126**, 2894–2904.
87 D. F. Sava, V. C. Kravtsov, F. Nouar, Ł. Wojtas, J. F. Eubank and M. Eddaoudi, *J. Am. Chem. Soc.*, 2008, **130**, 3768–3770.
88 M. Eddaoudi and Y. Liu, *US Pat.*, US 2006287190, 2006.
89 M. D. Foster and M. M. J. Treacy, A Database of Hypothetical Zeolite Structures: http://www.hypotheticalzeolites.net.
90 S. W. Keller, *Angew. Chem., Int. Ed. Engl.*, 1997, **36**, 247–248.
91 J. A. R. Navarro, E. Barea, J. M. Salas, N. Masciocchi, S. Galli, A. Sironi, C. O. Ania and J. B. Parra, *Inorg. Chem.*, 2006, **45**, 2397–2399.
92 Y.-Q. Tian, C.-X. Cai, Y. Ji, X.-Z. You, S.-M. Peng and G.-H. Lee, *Angew. Chem., Int. Ed.*, 2002, **41**, 1384–1386.
93 B. Wang, A. P. Côté, H. Furukawa, M. O'Keeffe and O. M. Yaghi, *Nature*, 2008, **453**, 207–211.
94 B. Wang, A. P. Côté, H. Furukawa, M. O'Keeffe and O. M. Yaghi, *Nature*, 2008, **453**, 207–211.
95 B. Liu, S. Li and J. Hu, *Am. J. PharmacoGenomics*, 2004, **4**, 263–276.
96 S.-S. Chen, M. Chen, S. Takamizawa, P. Wang, G.-C. Lv and W.-Y. Sun, *Chem. Commun.*, 2011, **47**, 4902–4904.
97 J. Zhang, T. Wu, C. Zhou, S. Chen, P. Feng and X. Bu, *Angew. Chem., Int. Ed.*, 2009, **48**, 2542–2545.
98 T. Wu, J. Zhang, C. Zhou, L. Wang, X. Bu and P. Feng, *J. Am. Chem. Soc.*, 2009, **131**, 6111–6113.
99 I. A. Baburin, B. Assfour, G. Seifert and S. Leoni, *Dalton Trans.*, 2011, **40**, 3796–3798.
100 X. Zhao, T. Wu, X. Bu and P. Feng, *Dalton Trans.*, 2011, **40**, 8072–8074.
101 M. Dinc, A. Dailly, Y. Liu, C. M. Brown, D. A. Neumann and J. R. Long, *J. Am. Chem. Soc.*, 2006, **128**, 16876–16883.
102 M. Dincă, W. S. Han, Y. Liu, A. Dailly, C. M. Brown and J. R. Long, *Angew. Chem., Int. Ed.*, 2007, **46**, 1419–1422.
103 W. Ouellette, K. Darling, A. Prosvirin, K. Whitenack, K. R. Dunbar and J. Zubieta, *Dalton Trans.*, 2011, **40**, 12288–12300.
104 S. Biswas, M. Maes, A. Dhakshinamoorthy, M. Feyand, D. E. De Vos, H. Garcia and N. Stock, *J. Mater. Chem.*, 2012, **22**, 10200–10209.
105 K. Sumida, S. Horike, S. S. Kaye, Z. R. Herm, W. L. Queen, C. M. Brown, F. Grandjean, G. J. Long, A. Dailly and J. R. Long, *Chem. Sci.*, 2010, **1**, 184–191.
106 V. Colombo, S. Galli, H. J. Choi, G. D. Han, A. Maspero, G. Palmisano, N. Masciocchi and J. R. Long, *Chem. Sci.*, 2011, **2**, 1311–1319.
107 A. Demessence, D. M. D'Alessandro, M. L. Foo and J. R. Long, *J. Am. Chem. Soc.*, 2009, **131**, 8784–8786.
108 Y.-X. Tan, Y.-P. He and J. Zhang, *Chem. Commun.*, 2011, **47**, 10647–10649.
109 L. Xie, S. Liu, C. Gao, R. Cao, J. Cao, C. Sun and Z. Su, *Inorg. Chem.*, 2007, **46**, 7782–7788.
110 S. Ma, X.-S. Wang, D. Yuan and H.-C. Zhou, *Angew. Chem., Int. Ed.*, 2008, **47**, 4130–4133.
111 S. Das, H. Kim and K. Kim, *J. Am. Chem. Soc.*, 2009, **131**, 3814–3815.
112 S. Ma, D. Yuan, X.-S. Wang and H.-C. Zhou, *Inorg. Chem.*, 2009, **48**, 2072–2077.
113 S. Ma, D. Yuan, J.-S. Chang and H.-C. Zhou, *Inorg. Chem.*, 2009, **48**, 5398–5402.

114 K. Sumida, D. L. Rogow, J. A. Mason, T. M. McDonald, E. D. Bloch, Z. R. Herm, T.-H. Bae and J. R. Long, *Chem. Rev.*, 2012, **112**, 724–781.
115 Z. Zhang, Z.-Z. Yao, S. Xiang and B. Chen, *Energy Environ. Sci.*, 2014, **7**, 2868–2899.
116 G. D. Pirngruber, L. Hamon, S. Bourrelly, P. L. Llewellyn, E. Lenoir, V. Guillerm, C. Serre and T. Devic, *ChemSusChem*, 2012, **5**, 762–776.
117 P. L. Llewellyn, S. Bourrelly, C. Serre, A. Vimont, M. Daturi, L. Hamon, G. De Weireld, J.-S. Chang, D.-Y. Hong, Y. Kyu Hwang, S. Hwa Jhung and G. Férey, *Langmuir*, 2008, **24**, 7245–7250.
118 P. Nugent, Y. Belmabkhout, S. D. Burd, A. J. Cairns, R. Luebke, K. Forrest, T. Pham, S. Ma, B. Space, Ł. Wojtas, M. Eddaoudi and M. J. Zaworotko, *Nature*, 2013, **495**, 80–84.
119 O. Shekhah, Y. Belmabkhout, Z. Chen, V. Guillerm, A. Cairns, K. Adil and M. Eddaoudi, *Nat. Commun.*, 2014, **5**, 4228.
120 W. Lu, J. P. Sculley, D. Yuan, R. Krishna, Z. Wei and H.-C. Zhou, *Angew. Chem., Int. Ed.*, 2012, **51**, 7480–7484.
121 V. Guillerm, Ł. J. Weseliński, M. Alkordi, M. I. H. Mohideen, Y. Belmabkhout, A. J. Cairns and M. Eddaoudi, *Chem. Commun.*, 2014, **50**, 1937–1940.
122 A. M. Fracaroli, H. Furukawa, M. Suzuki, M. Dodd, S. Okajima, F. Gándara, J. A. Reimer and O. M. Yaghi, *J. Am. Chem. Soc.*, 2014, **136**, 8863–8866.
123 R. Luebke, Ł. J. Weseliński, Y. Belmabkhout, Z. Chen, Ł. Wojtas and M. Eddaoudi, *Cryst. Growth Des.*, 2014, **14**, 414–418.
124 R. Luebke, J. F. Eubank, A. J. Cairns, Y. Belmabkhout, Ł. Wojtas and M. Eddaoudi, *Chem. Commun.*, 2012, **48**, 1455–1457.
125 J.-S. Qin, D.-Y. Du, W.-L. Li, J.-P. Zhang, S.-L. Li, Z.-M. Su, X.-L. Wang, Q. Xu, K.-Z. Shao and Y.-Q. Lan, *Chem. Sci.*, 2012, **3**, 2114–2118.
126 Y. Liu, V. C. Kravtsov, D. A. Beauchamp, J. F. Eubank and M. Eddaoudi, *J. Am. Chem. Soc.*, 2005, **127**, 7266–7267.
127 M. Eddaoudi, J. F. Eubank, Y. Liu, V. Ch. Kravtsov, R. W. Larsen and J. A. Brant, in *Studies in Surface Science and Catalysis*, ed. R. Xu, Z. Gao, J. Chen and W. Yan, Elsevier, 2007, vol. 170, pp. 2021–2029.
128 Y. Liu, V. Kravtsov, R. D. Walsh, P. Poddar, H. Srikanth and M. Eddaoudi, *Chem. Commun.*, 2004, 2806–2807.
129 M. H. Alkordi, J. A. Brant, Ł. Wojtas, V. C. Kravtsov, A. J. Cairns and M. Eddaoudi, *J. Am. Chem. Soc.*, 2009, **131**, 17753–17755.
130 M. H. Alkordi, J. L. Belof, E. Rivera, Ł. Wojtas and M. Eddaoudi, *Chem. Sci.*, 2011, **2**, 1695–1705.
131 Y. Liu, V. C. Kravtsov and M. Eddaoudi, *Angew. Chem., Int. Ed.*, 2008, **47**, 8446–8449.
132 F. Nouar, J. Eckert, J. F. Eubank, P. Forster and M. Eddaoudi, *J. Am. Chem. Soc.*, 2009, **131**, 2864–2870.
133 M. H. Alkordi, Y. Liu, R. W. Larsen, J. F. Eubank and M. Eddaoudi, *J. Am. Chem. Soc.*, 2008, **130**, 12639–12641.
134 S.-T. Zheng, F. Zuo, T. Wu, B. Irfanoglu, C. Chou, R. A. Nieto, P. Feng and X. Bu, *Angew. Chem., Int. Ed.*, 2011, **50**, 1849–1852.
135 F. Nouar, J. F. Eubank, T. Bousquet, Ł. Wojtas, M. J. Zaworotko and M. Eddaoudi, *J. Am. Chem. Soc.*, 2008, **130**, 1833–1835.
136 J. F. Eubank, F. Nouar, R. Luebke, A. J. Cairns, Ł. Wojtas, M. Alkordi, T. Bousquet, M. R. Hight, J. Eckert, J. P. Embs, P. A. Georgiev and M. Eddaoudi, *Angew. Chem., Int. Ed.*, 2012, **51**, 10099–10103.
137 V. Guillerm, D. Kim, J. F. Eubank, R. Luebke, X. Liu, K. Adil, M. S. Lah and M. Eddaoudi, *Chem. Soc. Rev.*, 2014, **43**, 6141–6172.
138 V. Guillerm, Ł. J. Weseliński, Y. Belmabkhout, A. J. Cairns, V. D'Elia, Ł. Wojtas, K. Adil and M. Eddaoudi, *Nat. Chem.*, 2014, **6**, 673–680.
139 Y. Zou, M. Park, S. Hong and M. S. Lah, *Chem. Commun.*, 2008, 2340–2342.
140 G. Barin, V. Krungleviciute, D. A. Gomez-Gualdron, A. A. Sarjeant, R. Q. Snurr, J. T. Hupp, T. Yildirim and O. K. Farha, *Chem. Mater.*, 2014, **26**, 1912–1917.
141 D. F. Sava, V. C. Kravtsov, J. Eckert, J. F. Eubank, F. Nouar and M. Eddaoudi, *J. Am. Chem. Soc.*, 2009, **131**, 10394–10396.
142 X. Zhao, T. Wu, S.-T. Zheng, L. Wang, X. Bu and P. Feng, *Chem. Commun.*, 2011, **47**, 5536–5538.
143 K. Koh, A. G. Wong-Foy and A. J. Matzger, *Angew. Chem., Int. Ed.*, 2008, **47**, 677–680.
144 X.-S. Wang, S. Ma, D. Sun, S. Parkin and H.-C. Zhou, *J. Am. Chem. Soc.*, 2006, **128**, 16474–16475.
145 P. Horcajada, H. Chevreau, D. Heurtaux, F. Benyettou, F. Salles, T. Devic, A. Garcia-Marquez, C. Yu, H. Lavrard, C. L. Dutson, E. Magnier, G. Maurin, E. Elkaim and C. Serre, *Chem. Commun.*, 2014, **50**, 6872–6874.
146 A. Sonnauer, F. Hoffmann, M. Fröba, L. Kienle, V. Duppel, M. Thommes, C. Serre, G. Férey and N. Stock, *Angew. Chem., Int. Ed.*, 2009, **48**, 3791–3794.
147 M. Latroche, S. Surblé, C. Serre, C. Mellot-Draznieks, P. L. Llewellyn, J.-H. Lee, J.-S. Chang, S. H. Jhung and G. Férey, *Angew. Chem., Int. Ed.*, 2006, **45**, 8227–8231.
148 P. Horcajada, T. Chalati, C. Serre, B. Gillet, C. Sebrie, T. Baati, J. F. Eubank, D. Heurtaux, P. Clayette, C. Kreuz, J.-S. Chang, Y. K. Hwang, V. Marsaud, P.-N. Bories, L. Cynober, S. Gil, G. Férey, P. Couvreur and R. Gref, *Nat. Mater.*, 2010, **9**, 172–178.
149 L. M. Rodriguez-Albelo, A. R. Ruiz-Salvador, D. W. Lewis, A. Gomez, P. Mialane, J. Marrot, A. Dolbecq, A. Sampieri and C. Mellot-Draznieks, *Phys. Chem. Chem. Phys.*, 2010, **12**, 8632–8639.
150 L. M. Rodriguez-Albelo, A. R. Ruiz-Salvador, A. Sampieri, D. W. Lewis, A. Gómez, B. Nohra, P. Mialane, J. Marrot, F. Sécheresse, C. Mellot-Draznieks, R. Ngo Biboum, B. Keita, L. Nadjo and A. Dolbecq, *J. Am. Chem. Soc.*, 2009, **131**, 16078–16087.
151 L. Sun, H. Xing, Z. Liang, J. Yu and R. Xu, *Chem. Commun.*, 2013, **49**, 11155–11157.
152 O. Shekhah, A. Cadiau and M. Eddaoudi, *CrystEngComm*, 2015, DOI: 10.1039/C4CE01402B.